SABINE • NECHES
NAVIGATION DISTRICT
Our commitment runs deep

Sabine Neches Navigation Improvement Project Integrated Section 203 Feasibility Report and Environmental Assessment

Appendix A Attachment 5

Vessel Effects Modeling Report

February 2026

Executive Summary

Hydrodynamic modeling of the Sabine-Neches Waterway (SNWW) was performed to support a Section 203 Integrated Feasibility Report for a proposed channel improvement project (Project). A channel deepening project (SNWW Channel Improvement Project) is currently under construction. The modeling performed in this effort is focused on channel widening that is not included in the channel deepening project. The overall modeling effort for the Section 203 Integrated Feasibility Report includes two-dimensional modeling of hydrodynamics associated with daily tides, storm surge events, hydrodynamic modeling of vessels in the SNWW, and three-dimensional modeling of hydrodynamics to assess water quality changes. This report discusses vessel effects modeling.

Modeling was performed using Adaptive Hydraulics Model System (AdH) developed by the Coastal and Hydraulics Laboratory (CHL) of the U.S. Army Corps of Engineers (USACE). Model meshes were developed to cover the entire project length as well as surrounding areas including Sabine Lake and surrounding marsh inlets where water may flow in and out during vessel transit events. Modeling focused on a single vessel in the Suezmax vessel class.

Six channel configurations were considered for the modeling: (1) Existing Conditions (EC), (2) Future without Project (FWOP) representing the channel deepening without the proposed widening, (3) Future with Project Full Build (FWPFB) which included the largest considered widening width and extent, and three smaller widening variations referred to as (4) Alternative 1 (ALT1), (5) Alternative 2 (ALT2), and (6) Alternative 3 (ALT3). The EC model was used for model calibration and the primary model (base to plan) comparisons were made between the FWOP and FWP conditions to capture changes that could occur as a result of the proposed channel improvements. Similarly, ALT1, ALT2, and ALT3 were compared to FWOP to evaluate base to plan changes.

Vessel modeling was performed to assess changes to drawdown and return current associated with transiting vessels, which can be related to bank erosion. The EC model runs were also part of the comparison but largely focused on model calibration and validation. Results of the modeling showed small changes in the return current if the vessel was traveling at the same speed in the FWOP, FWPFB, ALT1, ALT2, and ALT3 conditions. Modeling was performed for vessel transiting faster in the proposed channel, but these results are not presented because the local harbor pilots have stated they will restrict vessel speed. Overall, because the proposed widening does not increase drawdown and return current compared to FWOP, it is also not expected to cause increased bank erosion. Even though vessel hydrodynamics are not expected to increase, chronic bank erosion already exists along portions of the SNWW in areas without shoreline protection, or with inadequate shore protection. Previous studies have largely attributed this erosion to the historical vessel traffic up to present.

Table of Contents

List of Figures

List of Tables

1 Introduction

The Sabine-Neches Waterway (SNWW) provides a valuable avenue for waterborne commerce to transit between the Gulf of Mexico and the inland ports. The SNWW navigation channels are significantly deeper than the natural channels and tend to concentrate tidal current flows. These deeper navigation channels provide a conduit for saltwater to penetrate further into the inland system during elevated water levels on the coast. Therefore, it is important to study the effects of any changes to the SNWW channel configurations on system hydrodynamics and circulation.

The Sabine-Neches Navigation District (SNND) is conducting a study of potential channel improvements to the SNWW to be used for preparing a Section 203 Integrated Feasibility Report and appropriate environmental analyses. These improvements are in addition to the U.S. Army Corps of Engineers (USACE) channel improvement project (SNWW CIP) that is currently under construction to reconfigure and deepen the existing channel. The purpose of the new evaluation is to weigh the relevant factors related to widening portions of the navigation channel to increase vessel traffic efficiency and navigation safety along the SNWW in conjunction with the expanded vessel sizes allowed by the current deepening improvements. In this context, vessel traffic efficiency and navigation safety refer to vessel meetings that allow two-way traffic in the SNWW.

This technical report documents the numerical modeling performed for analysis of hydrodynamics related to transiting vessels and is developed to serve as a standalone document. Relative change in wave height/current speed from this report can be used as a proxy for bank erosion analysis and will also help generate portions of the Engineering Appendix for the Section 203 Integrated Feasibility Report.

The general project area and channel reaches considered for widening are shown in Figure 1-1 in relation to channel stationing shown at 10,000 ft increments. The proposed widening reaches shown in the figure represent all the potential widening locations considered, although alternatives are also considered for widening at only select locations.

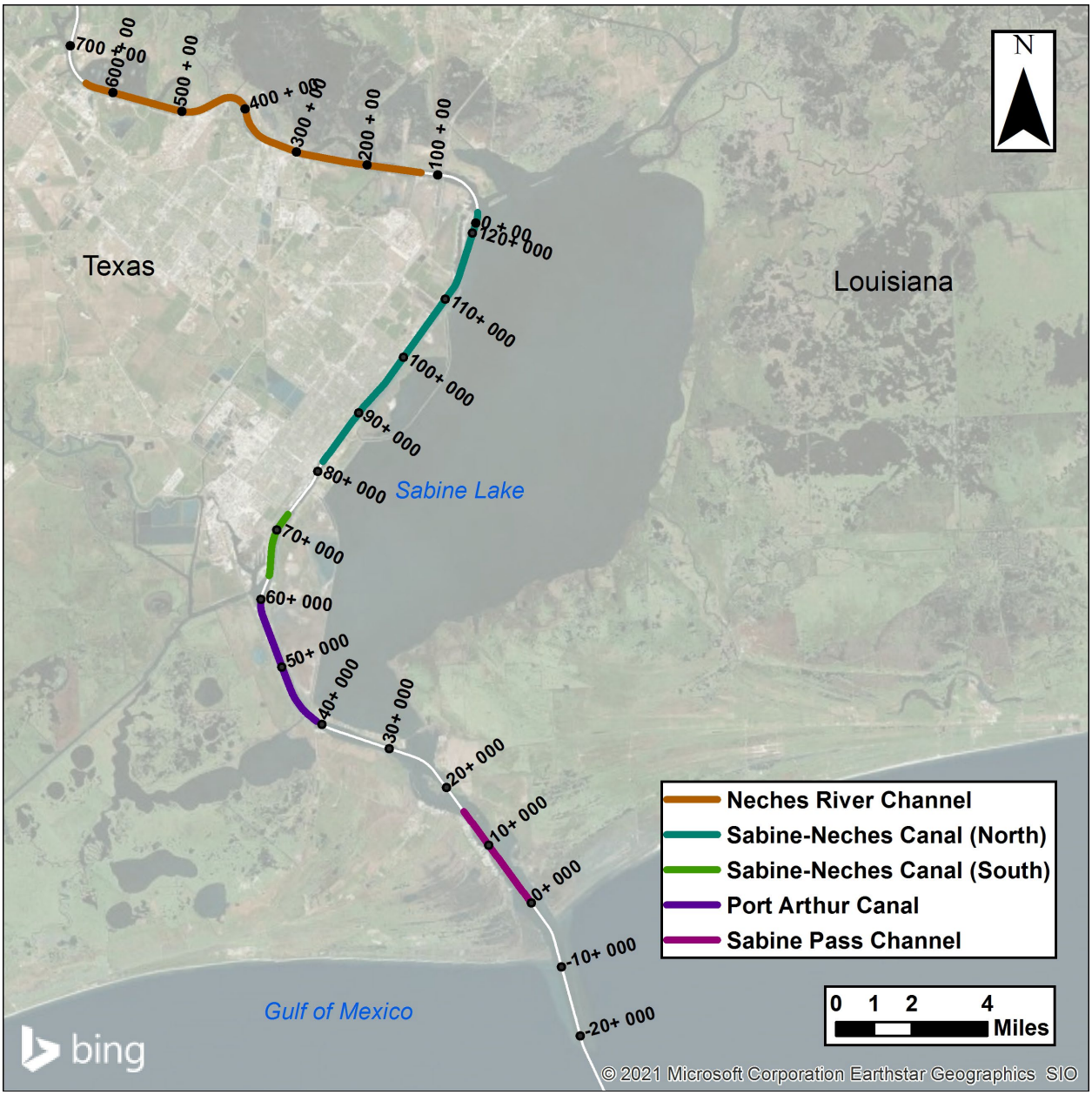

Figure 1-1
SNWW Locations Considered for Widening

Note: The color coding does not capture the full extent of each reach; rather, it refers to the name of the reach where each of the widening areas are considered.

1.1 Modeling Scope

An analysis was performed by HDR to examine the influence of widening portions of the SNWW on vessel generated hydrodynamics. This analysis used USACE's Adaptive Hydraulic Modeling system (AdH) to simulate vessels transiting within the existing channel and proposed channel geometries. Model results for each of these conditions were intercompared along the length of the channel based on peak vessel generated hydrodynamics. These model simulations all focused on

the Suezmax vessel class, which is the largest size expected to use the future channel. Vessel size was kept constant between existing and future conditions to isolate hydrodynamic changes resulting from channel modifications, with only a single parameter (either draft or speed) adjusted between comparisons. The choice of draft and speed was informed by theoretical limits determined from representative channel cross-section geometries and considered observed vessel speeds in the existing channel as well as previous studies. Model calibration/validation was based on field measurements of passing vessel hydrodynamics. Field measurements captured several Aframax class vessels and therefore these vessels/events were used for calibration. Several additional simulations were also compared for future with-project conditions including a relative sea level change scenario. This document describes methodology and results of the vessel analysis and discusses the field data collection effort performed to supplement the numerical modeling effort.

While the proposed channel widening will allow vessel meetings where they are not able to meet in the current channel width, this modeling effort is focused on the vessel hydrodynamics from a single vessel transiting the channel. Additional discussion of vessel meetings in the proposed channel is provided in Section 1.2 compared to hydrodynamics of a single vessel.

1.2 Vessel Hydrodynamics

In confined shipping channels such as the SNWW, vessel transits produce significant fluctuations in currents and water levels. These dynamic water levels and currents can adversely affect moored vessels along the channel, generate bottom stresses linked to channel shoaling, and contribute to channel bank erosion. The hydrodynamic response from transiting vessels in confined channels is characterized, in order as if an individual was watching these events from the channel bank, by a slight rise in the water level referred to as the "bow wave," followed by a depression in the water surface known as "drawdown" and an associated "return current" that moves in the opposite direction relative to the vessel, and finally a sudden increase in water level from the drawdown. A schematic depiction of the process is shown in Figure 1-2. In some cases, there will be a surge after the drawdown where the water level exceeds the still water level, or the water level before ship effects, as seen in Figure 1-2. The total change from the trough of the drawdown to the crest of the surge is commonly known as a "transverse stern wave" (TSW), labeled as "Stern Wave" in the figure.

Drawdown, return current, and the stern wave all extend laterally on both sides of the vessel. Longitudinally (in the direction the vessel is travelling) the wavelength of the drawdown and return current is approximately the length of the vessel. The surge is more prominent along the outside of the channel in shallow water. A review by Maynord (2003) suggests TSWs with Froude (Fr) numbers less than 0.75 will not have a surge (i.e., the water level will not increase above the still water level after the drawdown), TSWs with Fr numbers between 0.75 and 1.1 will create an undular bore or surge that has not broken, and Fr numbers greater than 1.1 will create a broken bore surge. An example of a vessel-induced breaking bore near the bank of the SNWW is given in Figure 1-3.

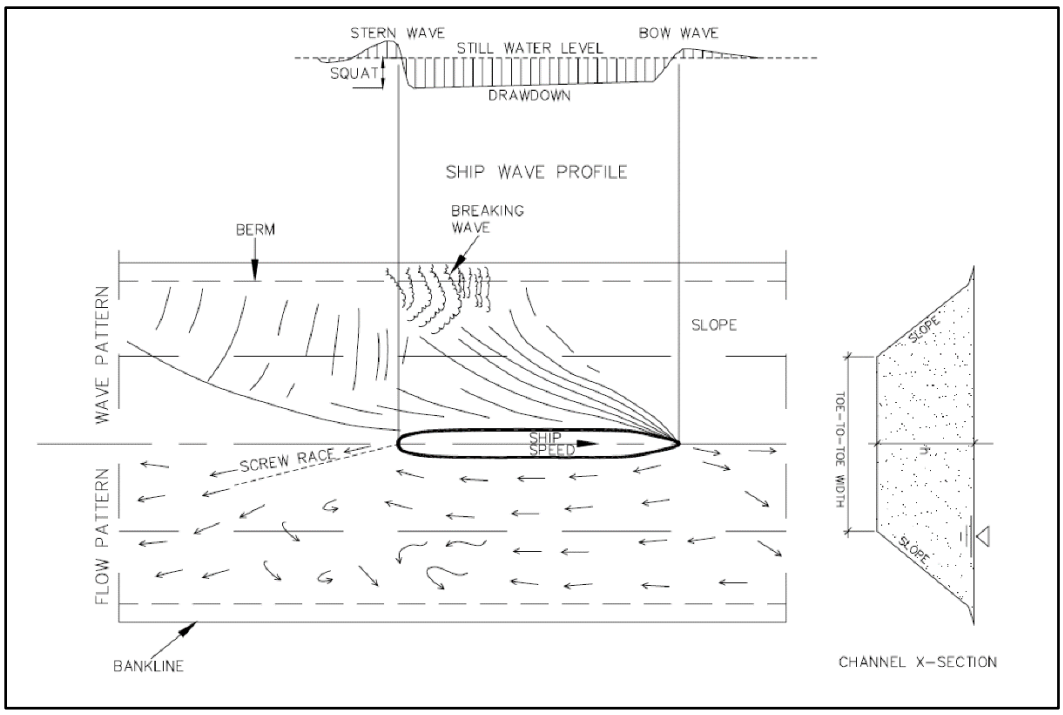

Figure 1-2
Ship Waves and Flow Pattern in a Canal from EM 1110-2-1613.

Figure 1-3
Photo of Vessel-Induced Breaking Bore Along the SNWW Bank.

The magnitude of these hydrodynamic responses caused by vessel transits is most affected by the speed of the vessel, and the relative size of the channel cross-section to the vessel cross-section (blockage-ratio). Schijf and Janssen (1953) derived formulas to approximate drawdown and surge based on the Bernoulli equation and the conservation of mass. These formulas are commonly referred to as the "Schijf equations." In addition to estimating the hydrodynamics in the channel caused by vessel transit, the channel cross-section itself imposes limits to vessel size, draft, and speed, which can be used to estimate the theoretical maximum speed attainable (known as the limiting speed). The actual maximum speed is determined by the vessel pilot based on safety and other considerations. Previous observations of vessel traffic in the SNWW presented in Maynord (2003) showed unloaded vessels traveled at 80-85 percent limiting speed and loaded vessels at 75-80 percent limiting speed. The theoretical limiting speed concept was applied here to inform choices of run parameters. Further details about the Schijf equations are presented in Section 4.5.

When two vessels meet, the hydrodynamic response from the vessels act independently of each other for nearly their entire transit through the channel and only interact at one discrete location where the flow patterns can partially counteract each other (Schijf, 1953). The mechanism for this cancelation is due to opposition of the return currents directions, which in turn counteracts the magnitude of the drawdown. Therefore, the effect of the vessel transit on the adjacent banks can primarily be based on a single vessel. All the momentum in the wakes is traveling in the same direction as the vessel creating the wake and continues with the vessel after the passing. Because of channel bank erosion is dependent of the cumulative effects of vessel wakes, the hydrodynamics from a single vessel along the entire channel is more relevant than the short duration wake at an arbitrary meeting location. Further, the total number of vessels calling on the SNNW is not expected to increase as a result of the channel widening, and the number of larger vessels passing will be less than one (1) per day at the most heavily trafficked locations. For these reasons and consistent with other channel improvement feasibility studies (USACE, 2008, 2019), this report does not focus on the effects of two vessels meeting (i.e., passing side-by-side) within the channel.

1.3 Units and Datums

All models applied in this study were developed using International units, however, following common practice all channel depths and widths are presented in English units. Therefore, there is a mix of feet (ft) and meters (m) presented in this report. Similarly, vessel speeds are presented in both nautical miles per hour (kts) and meters per second (m/s). A few instances of shoaling volumes are also presented in the cubic yards, also common practice. For datums, all models are referenced to NAD83 Texas State Plane South Central horizontal coordinate system and the North Atlantic Vertical Datum of 1988 (NAVD88). The depths for the channel configurations detailed in Section 3 are defined relative to mean lower low water (MLLW) but were converted to NAVD88 using VDatum software during model scatter development.

2 Previous Studies

SNWW went through the Feasibility Study process in 2003-2011 for a deepening project where the authorized depth was increased from an elevation of -40 ft mean lower low water (MLLW) to -48 ft MLLW. This previous study (USACE, 2016) provides a good reference for vessel modeling performed in SNWW. The Feasibility Study related to vessel hydrodynamics can be broken into the following two main reports.

2.1 Ship Effects Before and After Deepening of Sabine-Neches Waterway, Port Arthur, Texas, Maynord (2003)

Maynord's report looked at vessel effects in the SNWW that may lead to bank erosion before and after modifications to the navigation channel as part of the Channel Improvement Project. The study included both a field measurement component and a modeling component using HIVEL2D (the predecessor to the AdH model used herein). Two scenarios were investigated, 1) the "design ship" in the existing and proposed channels, and 2) a larger vessel in the proposed channel. The larger vessel represented a vessel that could transit the channel once it was deepened. Both scenarios were evaluated at two different cross-sections, "north site" and "south site," representative of sections of the Sabine-Neches Canal and Port Arthur Canal, respectively. The north site section was evaluated for deepening only and remained at 400 ft bottom width, while the south site was evaluated for both deepening and widening from 500 ft to 700 ft. Although widening was evaluated, it was not included in the recommended plan for the SNWW CIP. The study used the TSW as a proxy to indirectly evaluate bank erosion. Results were most sensitive to ship speed, and it was found that the TSW height would increase by 10 to 35 percent for the range of speeds considered for the proposed channel. The range of speeds modeled for the 48 ft draft Suezmax vessel was 6.3 kts to 6.8 kts for the 400 ft width north site section of deepened channel, which equates to 75 to 80 percent limiting speed, respectively. For the same vessel at the south site, the modeled 75 to 80 percent limiting speeds were faster (8.3 to 8.9 kts, respectively) because of the larger area of the proposed channel. The report concluded that for both existing and proposed channels, small changes in vessel speed can result in large changes in TSW. Additionally, the shallow area between the channel and the bank, referred to as a berm, may amplify the drawdown and surge and hence the TSW.

2.2 Sabine-Neches Navigation Channel Improvement Project, Final Engineering Appendix, USACE (2008)

USACE published a Final Engineering Appendix in 2008 for the Sabine-Neches Waterway Channel Improvement Feasibility Study (2011)[1] to assess impacts to the SNWW from the proposed deepening. Engineering studies included ship simulations, erosion, and salinity investigations by the USACE's Engineer Research and Development Center (ERDC).

This work presented is an expansion of Maynord 2003 and includes additional focus on vessel speed and frequency occurrence. The objective was to quantify bank erosion caused by a vessel transiting in the SNWW navigation channels with and without changes to the existing channel conditions. The main findings reinforced the previous conclusions that ship speed is the most important parameter controlling TSW and associated bank erosion. Analysis was based at two cross-sections where historical bank recession estimates were 10-15 ft/yr. These recession rates were combined with historical ship traffic data to calibrate a bank erosion per ship estimate. These estimates were scaled based on the magnitude of shear stress for each vessel and the frequency of occurrence. Erosion per ship estimates were used together with future estimates of vessel traffic to predict changes to bank erosion rates. Their findings suggest that with project bank recession is less than without project bank recession. When comparing present erosion rates to future erosion rates, channel reaches where more channel cross-sectional area was added in the with-project

[1] Referred to as the Sabine Neches Navigation Channel Improvement Project in the Engineering Appendix.

conditions, were less likely to experience increase bank recession despite an increase in future vessel traffic.

3 Modeled Channel Configurations

The hydrodynamic modeling described in this report analyzes six channel configurations which are presented in this section. References to channel depth are based on the authorized depth relative to mean lower low water (MLLW). A summary of the configuration-specific widening locations and dimensions is provided in Table 3-1.

3.1 Channel Configuration 1: Existing Conditions

Referred to as Existing Conditions (EC), this configuration represents the channel conditions in place during the time of the data record used for model calibration (2018-2020 timeframe) prior to the start of the SNWW CIP construction. The authorized channel depth for this configuration is 40 ft below MLLW, although the conditions modeled are based on the available survey data and were not modified (see Section 4.2). This model condition will primarily serve as a model calibration/validation. This condition will also help qualify the cumulative changes predicted from the Future without Project (CIP Completed) and widening alternatives. Note the effects for the Future without Project (CIP Completed) condition were already captured in the 2011 CIP feasibility study (USACE, 2011).

3.2 Channel Configuration 2: Future without Project (SNWW CIP Completed)

Referred to as Future without Project or FWOP, this configuration represents the approved channel deepening to an authorized depth of 48 ft below MLLW (USACE, 2011). While this channel configuration is not yet completed, the SNWW CIP's new-start construction was funded in Fiscal Year (FY) 2019 by the Army Civil Works Program FY 2019 Work Plan (USACE, 2018a), and construction was initiated in 2020. The entire CIP is expected to take 7-10 years to complete construction.

3.3 Channel Configuration 3: Future with Project Full Build

Referred to as Future with Project Full Build or FWPFB, this channel configuration represents the largest combination of proposed widening measures. The authorized channel depth is 48 ft below MLLW, same as the FWOP. Figure 1-1 shows the locations of the widening features.

3.4 Channel Configuration 4: Alternative 1

Referred to as Alternative 1 or ALT1, this channel configuration includes widening to 500 ft (+100) reaches of the Sabine-Neches Canal and the Neches River Channel. Authorized depth remains 48 ft below MLLW.

3.5 Channel Configuration 5: Alternative 2

Referred to as Alternative 2 or ALT2, this channel configuration includes widening to 600 ft (+200) reaches of the Sabine-Neches Canal and the Neches River Channel. Authorized depth

remains 48 ft below MLLW. ALT2 focuses on widening in the same locations as ALT1, but increases the width by 100 ft.

3.6 Channel Configuration 6: Alternative 3

Referred to as Alternative 3 or ALT3, this channel configuration includes widening to 500 ft (+100) reaches of the Sabine-Neches Canal and the Neches River Channel and widening to 700 ft (+200) the Sabine Pass Channel and the Port Arthur Canal. ALT3 is the same as ALT1 in the Sabine-Neches Canal and Neches River Channel but also includes widening of the southern reaches.

Table 3-1
Widening Locations and Dimensions for the Six Channel Configurations

Reach	Station (Start)	Station (End)	Existing Condition (EC)	Future without Project (FWOP)	Future With Project Full Build (FWPFB)	Alternative 1 (ALT1)	Alternative 2 (ALT2)	Alternative 3 (ALT3)
Sabine Pass Channel	0+150	15+990	500 ft	500 ft	700 ft (same centerline)	No change to existing	No change to existing	700 ft (same centerline)
Port Arthur Canal	43+900	59+740	500 ft	500 ft				
Sabine Neches Canal (South)	63+500	72+700	400 ft	400 ft	600 ft (same western boundary; shift to east)	500 ft (same western boundary; shift to east)	600 ft (same western boundary; shift to east)	500 ft (same western boundary; shift to east)
Sabine Neches Canal (North)	81+510	35+00	400 ft	400 ft				
Neches River Channel[1]	122+40	640+00	400 ft	400 ft	600 ft (same western boundary; shift to east)	500 ft (same western boundary; shift to east)	600 ft (same western boundary; shift to east)	500 ft (same western boundary; shift to east)

[1] Around Station 623+00 in the Neches River Channel, expansion of Anchorage Basin 4 from 18 acres to 97 acres was initially considered and was included in modeled with-project configurations but was later eliminated from the final alternatives.

4 Model Setup

4.1 Model Description

AdH was applied for simulating vessel hydrodynamics in the SNWW. AdH is a water circulation modeling software developed by the Coastal and Hydraulics Laboratory (CHL) of the USACE that can incorporate moving vessels. AdH uses hydraulic flow dynamics to solve two-dimensional shallow water flows, including hydraulic processes caused by the movement of single or multiple vessels (Berger, Tate, Brown and Savant 2010). The model simulates a transiting vessel by applying a moving pressure field that displaces the equivalent volume of water as the modeled vessel. Vessel parameters can be specified including size, speed, and heading. The model is used to calculate time-dependent hydrodynamic parameters (water surface elevations and velocities) within the domain. An additional benefit of the model is the adaptive mesh capability, which further refines the mesh based on hydraulic criteria during the model run. This feature enhances model resolution where it is important without excessively increasing computational demand.

The other numerical modeling performed for the SNND proposed channel widening (documented in separate reports) was performed in MIKE21. The numerical modeling team at HDR is proficient in the use of MIKE21 for hydrodynamic modeling of tides and storm surge. However, while application of MIKE21 for vessel effects modeling is now being marketed by model developers, the application is new and the HDR has previously invested time into working with AdH to model vessel wakes. HDR has applied the AdH model to simulate vessel drawdown and return current in the Houston Ship Channel, SNWW, Corpus Christi Ship Channel, and additional locations, including several calibration exercises.

4.2 Bathymetry and Topography Data

Bathymetric and topographic elevation data in the vicinity of the existing navigation channel were retrieved from two sources:

1. National Oceanic and Atmospheric Administration (NOAA) “Online Data Access Viewer” in the form of the Continuously Updated Digital Elevation Model (CUDEM) Cooperative Institute for Research in Environmental Sciences (CIRES) at the University of Colorado (CIRES, 2014).
2. FEMA 2011 Texas Flood Study ADCIRC Mesh (FEMA, 2011).

The primary data set for the model elevation data is the NOAA CUDEM. This data set is a merged product of topography and bathymetry and is developed by NOAA to support different NOAA objectives such as inundation modeling. The CUDEM elevation data are provided with 3 meters (m) resolution horizontally. Each CUDEM dataset is accompanied by a metadata shapefile that describes the source data (date and special extent), where USACE hydrographic surveys were used for the SNWW navigation channel. Spot checks to USACE hydrographic surveys in the SNWW Navigation channel showed good qualitative agreement (depth differences approximately 1m). However, some areas in the CUDEMs lack quality source data (as shown by gaps in the metadata files), where there is high uncertainty and in the elevations. In particular, the bathymetry of the SNWW areas outside the navigation channel and the bank are not typically surveyed or well resolved on the NOAA navigation charts (also a CUDEM data source). Depths in rivers upstream of the USACE survey extents are also uncertain in the CUDEM data. For areas with good source

data, there may be small differences as a result of the CUDEM merging and processing, such as the low-pass median filter applied that covers approximately 50 m horizontally.

During the comprehensive review of the data, several areas of localized non-federal dredging were noted as not included in the NOAA CUDEM elevation data. In these areas, the elevation data were manually adjusted to capture the new berth dredging depths. Also, the model mesh and project limits extend beyond 30° north latitude, but the NOAA CUDEM data set does not. For the northern portion of the meshes where NOAA CUDEM data were not available, the mesh from the FEMA (2011) modeling was converted to elevation data and merged. The resolution of the elevation data from the FEMA (2011) modeling varied depending on the ADCIRC mesh resolution, but in general the resolution increased around areas of hydraulic significance. A depiction of the spatial extent of the elevation data sets applied geographically for mesh development is shown in Figure 4-1.

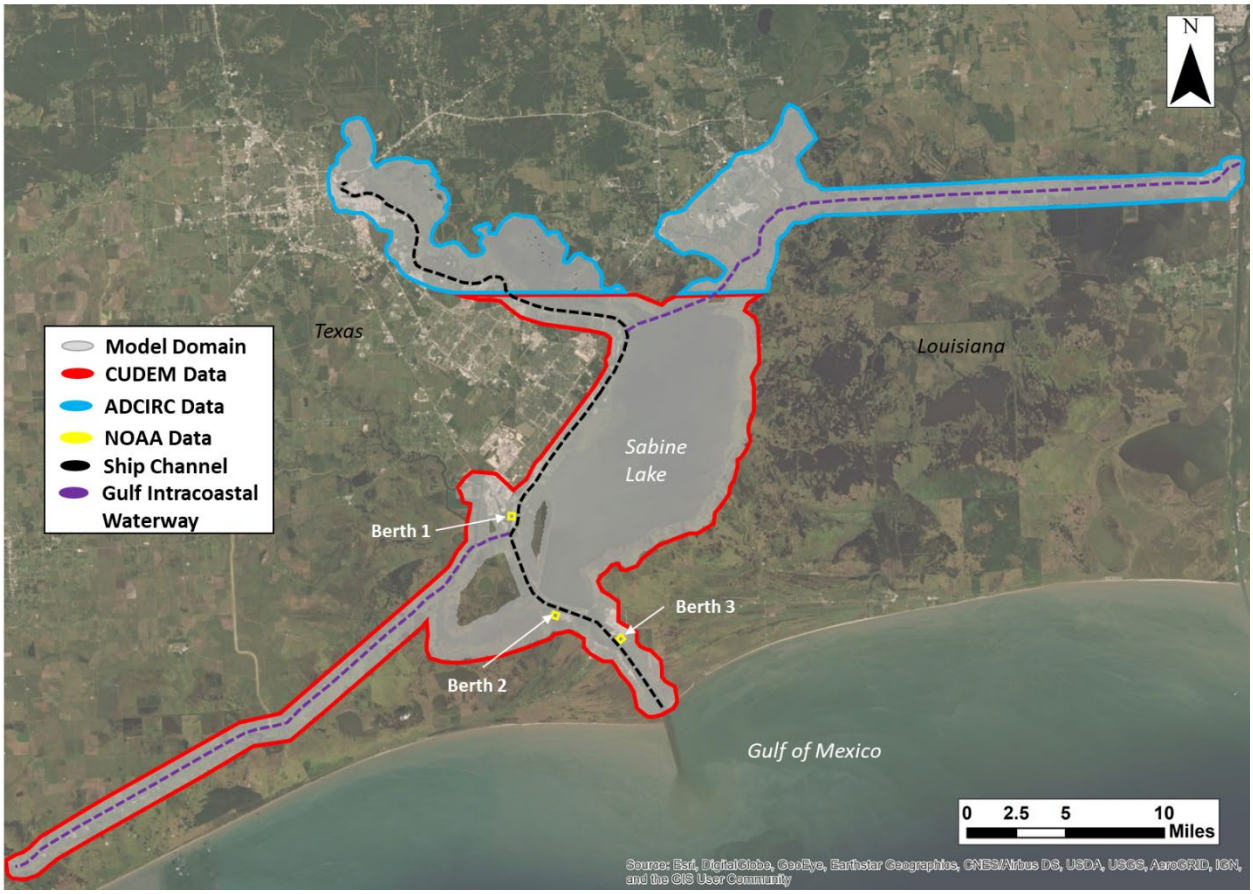

Figure 4-1
Elevation Source Data Summary

The various channel configurations for modeling are discussed in Section 3. For the EC modeling, primarily used as a calibration model, additional manipulation of the elevation data was not performed. For all future channel configurations, the elevation data were adjusted based on the proposed channel template, but elevation data beyond the impact of the proposed conditions were not modified. All modified channel configurations applied channel side slopes of 2H:1V, which is the design slope in the preliminary engineering phase. It is likely the channel slope will ultimately

begin to become shallower (i.e., less steep) after project construction. The same 2H:1V slope is used for the SNWW CIP as described in USACE (2011).

4.3 Model Mesh Development

The Surface-water Modeling System (SMS) software was used to generate meshes within the AdH simulations. Because it was not computationally feasible to cover the entire extent of the channel improvement project (approximately 40 miles) in a single mesh, three separate overlapping meshes were created as shown in Figure 4-2:

- North (red polygon)
- Central (green polygon)
- South (blue polygon)

These mesh files overlap horizontally so that modeled vessels and the corresponding hydrodynamics have time and space to ramp up before reaching the portion of the model domain used in the analysis. Figure 4-2 shows the geographical extents of the three model domains.

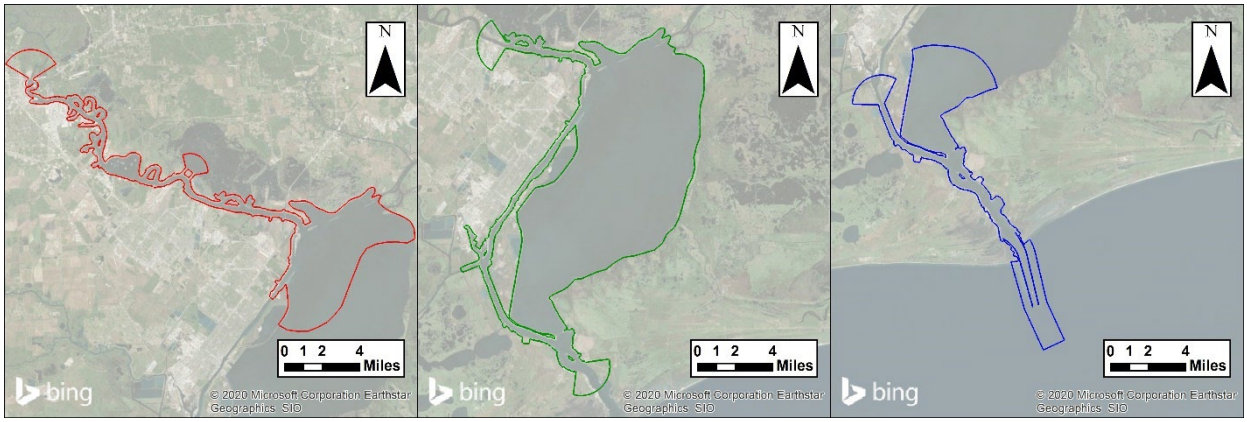

Figure 4-2
North, Central, and South Mesh Boundaries for AdH Modeling

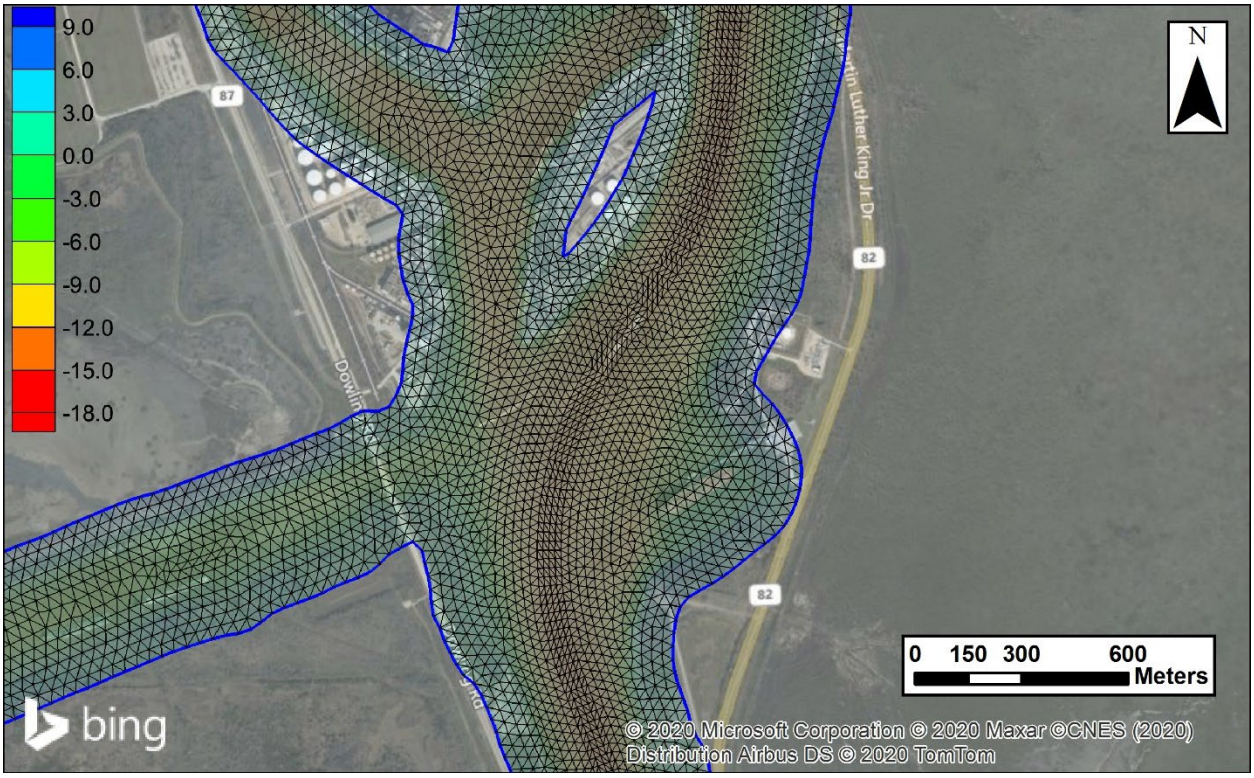

Figure 4-3
Central Mesh Resolution Near Taylor Bayou for FWPFB Channel Configuration

The meshes were refined along the vessel sailing path and along the channel to accurately resolve the vessel and channel improvement project configurations. A version of the north, central, and south meshes was developed for each of the channel configurations for a total of 18 meshes (6 channel configurations on each of the 3 meshes). Other than the elevations associated with the channel configurations, the element spacing and size was consistent between the meshes for the different channel configurations. An example segment of the central mesh is shown in Figure 4-3 near Taylors Bayou. The mesh surrounding the vessel sailing path has 25 meter (m) spacing along the lengthwise direction and 17 m in the transverse direction. The mesh development strategy was based on guidance from the AdH manual and relevant AdH technical papers with regards to the vessel size along the sailing path (Berger et al. 2010; Berger and Lee 2008, Hammack 2008). Outside the area immediately surrounding the vessel sailing path, the mesh element size expands gradually, but features additional refinements at areas of hydraulic importance such as adjacent channels, bathymetric shoals, and depressions that would affect the vessel hydrodynamics. Overall element side lengths ranged from 16 m to 900 m.

4.4 Mesh Convergence Test

A mesh convergence tests was performed by reducing the mesh element size along the channel centerline. Element size was reduced from 25 m to 10.3 m, while the model time step was kept at 2.5 s. The peak values of the modeled velocity (return current) and water level (drawdown) from the time series were compared at 12 points located on 2 shore normal transects. Each transect spanned between the edge of the channel and the bank. These time series comparisons showed a small reduction both in drawdown (~0.05 m) and return current (~0.07 m/s) on average for the

more refined mesh. There was one outlier in the comparison with larger differences, however, these differences resulted from changed mesh bathymetry (depth) after interpolation to the increased resolution mesh. Based on these time series comparisons, the 25 m longitudinal spacing along the channel was deemed sufficient and conservative because the more refined mesh slightly reduced drawdown and return current magnitudes.

4.5 Model Forcing and Boundary Conditions

4.5.1 Closed Boundary

A closed boundary was used for model simulations. This boundary type does not allow waves to enter the domain, and any outgoing waves are reflected into the domain. The model boundaries were placed at least 5 km beyond the vessel sailing path which was determined through review of the modeled water levels to be far enough from the channel and project areas such that reflected waves or artificial flow confinements would not impact the results.

4.5.2 Tides and Initial Water Level Conditions

Tidal forcing was not used in the vessel model due to the small tidal variations on the order of 1.0 ft to 1.5 ft in the region, and the much-shorter time scale for vessel-induced water motions (30 seconds to several minutes) compared to tides (6 to 12 hours). The water level was set at +0.43 m NAVD88 corresponding to the approximate 2020 mean sea level. The initial water level for the calibration and validation runs were set at +0.28 m NAVD88 and +0.32 NAVD88 respectively based on the observed tide at NOAA station 8770475 Port Arthur, TX at the time of the vessel transit. The initial condition did not include currents or waves within the model domain (i.e., still basin).

4.5.3 Sediment Transport

Sediment transport was not used in the vessel model.

4.5.4 Waves

No wave forcing was included in the model. Transiting vessel waves (transverse stern waves, but not diverging waves) were generated by the movement of vessels within the domain.

4.5.5 Salinity

Salinity was not included in the model.

4.5.6 Bottom Friction

Bottom friction was included to represent hydraulic processes more accurately. A constant Manning's coefficient of 0.02 was used throughout the domain and the kinematic viscosity of water was set to 1.139 E-6 m2/s. A model sensitivity analysis was performed to check the influence of Manning's coefficient on results as part of the model calibration in section 5. The sensitivity test showed these parameters had minimal influence on the results.

4.5.7 Wind Forcing

Wind forcing was not included in this model.

4.5.8 Other Forcing

Land above a maximum expected flood elevation or outside the area of interest was specified as a closed boundary. Elements within the boundaries flood and dry as water level varies.

4.5.9 Ship Forcing

Ships within the model are represented as pressure fields of the magnitude and dimension specified by the user. This is the same approach used by Maynord (2003) and is standard for AdH. A pre-run for each simulation was completed containing a stationary ship at its initial location to allow the water surface to assimilate to the pressure field and remove any artificial waves before ship movement. The pressure field representing the ship moves along a user defined path defined by a series of straight segments and horizontal curves. At model time zero the stationary ship (pressure field) begins to accelerate over an approximately 1,200-m segment until reaching a constant speed. Ship speeds and dimensions modeled for with and without project conditions are detailed in section 4.5 and those used for calibration and validation given in section 5.

4.6 Model Simulations

4.6.1 Modeled Vessel

Six transiting vessel model scenarios were developed using the AdH model; each consisted of one of the six channel configurations (i.e., EC, FWOP, FWPFB, ALT1, ALT2, ALT3) combined with a vessel size, draft, and speed. All six scenarios focused on the Suezmax vessel class which is the largest vessel class expected to use the deepened SNWW channel as presented in the Final Feasibility Report for the SNWW CIP (USACE 2011). This vessel size also matches the largest class used in Maynord 2003 and will allow general comparisons. The Suezmax vessel applied is approximately 135,000 DWT with further parameters detailed in Table 4-1. The Suezmax vessel was selected to model because it is the largest vessel expected to use the SNWW and cause the largest hydrodynamic effects (Maynord, 2003, USACE 2011). The Suezmax vessels are likely to be more frequent with further channel improvements, however, this vessel class was not observed during the calibration field observations and was not modeled for the calibration runs discussed in Section 5, which were in the smaller Aframax vessel class. The Suezmax ship class was kept constant for all model scenarios, however, the draft and speed varied for each modeled scenario. In general, a deeper and wider channel will reduce vessel effects for the same vessel size, draft, and speed as explained by the physics of the Schijf equations (See section 1.2 and limit speed below). Alternatively, the deepening and widening allows for an increase in speed or draft without necessarily increasing vessel effects. Further details of the selection of vessel speed and draft for each channel condition are discussed next.

4.6.2 Vessel Parameters

Vessel hydrodynamics are sensitive to the vessel parameters and the channel and waterway geometry. Increases in vessel draft, vessel length, vessel beam, and vessel speed all increase the vessel hydrodynamic effects on the waterway. Increases in the waterway cross-section (e.g., deepened or widened channels) generally decrease the vessel hydrodynamic effects. Selection of the modeled vessel speeds and drafts attempted to hold as many variables constant between the simulated channel conditions as possible while also using the modeling to assess the potential changes in hydrodynamics that would result from the proposed widening. Doing so required consideration of any potential changes in the vessel parameters that may occur due to the proposed

channel widening alternatives. Vessel size will not increase from the FWOP channel depth (48 ft) to the FWP channel depth (48 ft), but the widening would allow two-way traffic or vessel meeting (not modeled with AdH in this report). A discussion of vessel meeting is given in Section 1.2. Given a deeper or wider channel, vessels tend to increase draft (cargo) or transit at a faster speed. The FWOP (48 ft) and FWP (48 ft) conditions both have a deeper channel than the EC (40 ft) allowing vessels with deeper drafts to transit the waterway.

The modeled vessel drafts were selected based on maintaining safe under keel clearance. Typically, vessels transiting Texas ports maintain 4 to 6 ft of under keel clearance. The productions run vessel had a 36-ft draft in the EC and 44-ft draft for the future conditions. A precise vessel path within the channel was critical for maintaining under keel clearance for the Suezmax vessel in EC.

The modeled vessel speed in the EC channel was based on 90 percent of the theoretical "limit speed." Although most vessels will travel near 75 to 85 percent of the limiting speed (Maynord, 2003), use of this upper limit for speed is consistent with bank protection design guidelines (PIANC, 1987). This theoretical basis was used for determining design speeds since no data are available for the deepened and widened channel. These speeds are consistent with the largest (presumably fully loaded) vessels transiting the channel in its existing condition. Details about limiting speed calculations are discussed in the next section. A constant vessel speed of 8 knots (kts) was determined based on the 36-ft Suezmax vessel in the EC. This 8-kt vessel speed was kept constant and combined with each of the channel conditions to form the first three modeled scenarios, which are summarized in Figure 4-5 and Table 4-1. The equations used to develop the limit speeds are presented in the next section, and an example is provided for the FWOP simulated condition.

As an additional assessment of the vessel speed to be used in the model, AIS data for vessels larger than 500 ft was gathered from [https://marinecadastre.gov/ais/] during the period from 01/01/2020 to 12/31/2020. This source reports either the maximum vessel draft or the static vessel draft but does not specify which; therefore, draft was not considered in the assessment. The gathered data was analyzed to determine the percent exceedance for vessel speeds along the length of the channel and the results are plotted in Figure 4-4.

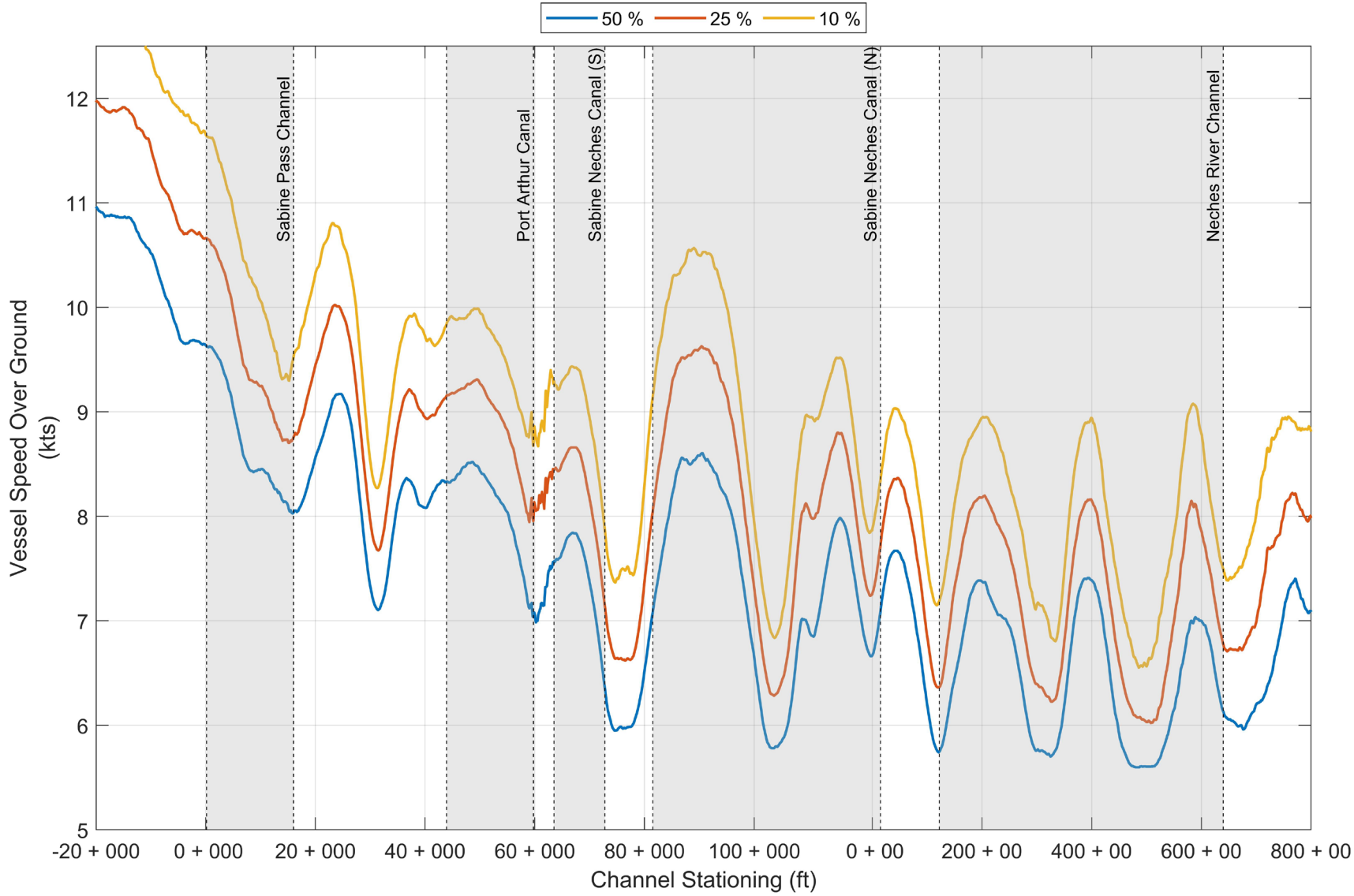

Figure 4-4
Vessel Transit Speeds in the SNWW Observed From 2020 AIS Data for Vessel Lengths Greater than 500 ft And Vessel Widths Greater Than 100 ft

The horizontal axis of the figure shows the channel stationing with the vessel speed plotted on the vertical axis. The different lines refer to the vessel speed exceeded in 50%, 25%, and 10% of the observations. For each specific channel stations, the analysis included AIS records located within 60 m radius of the channel centerline and at least 5 kts speed. From the figure, the vessel speeds generally decrease as vessels travel further inland on the waterway. The reason for the fluctuations between faster and slower speeds along the channel is not completely clear. The slower areas roughly correspond to reaches that feature ship berths or narrower areas of the SNWW. The intermittent slower speeds may be from vessel entering or exiting berths, from ship slowing to reduce hydrodynamics on nearby moored vessels, or from increased "resistance" as explained by the Schijf equations in the narrower sections of the channel. Because the mechanism for the speed fluctuations is not known, a constant speed was modeled for all model simulations to facilitate direct comparisons between existing and proposed conditions. For the EC a model vessel speed of 8 kts was chosen and in reviewing the figure falls within the observed vessel speeds for most of the channel length. Note that the information obtained from AIS is only applicable to the EC. Comparing AIS speeds for different vessel sizes (not shown), there is an approximate 0.5-kt reduction in speed for the largest vessel compared to all vessels above 500 ft length and 100 width as shown in Figure 4-4. Because the AIS data did not specify partially loaded draft, the percent limiting speed could not be determined for the downloaded vessel traffic data.

Table 4-1
AdH Model Vessel Input Parameters Simulated with Each Channel Configuration

Simulated Condition	Description	Length (ft)	Beam (ft)	Draft (ft)	Speed (kts)	% Limit Speed
EC (2019)	Existing Conditions (channel conditions in place in the 2018 to 2020 timeframe)	900	164	36	8	90
FWOP	Future Without Project (channel deepening project completed)	900	164	44	8	89
FWPFB **ALT1** **ALT2** **ALT3**	Future With Project (channel widening scenarios)	900	164	44	8	74

The analysis of the model scenarios is broken down into paired comparisons summarized as follows and illustrated in Figure 4-5 for a typical channel cross-section:

- Comparison A: Increasing the depth of the channel and the draft of the vessel (EC to FWOP) with the same 8 kts vessel speed. This vessel speed is approximately 90 percent of the limit speed for EC and FWOP.
- Comparison B: Increasing the width of the channel (FWOP to FWP) using the same vessel speed and draft. The wider channel increases the limit speed such that 8 kts is 74 percent. Comparison B is used to describe comparisons between FWOP and each of the FWP scenarios, i.e., FWPFB (Comparison "B") and ALT1 , ALT2, and ALT3 (Comparisons "B1 to B3"). While it is physically possible for vessels to transit faster

based on the limit speed, communications with the SNND Pilots indicated that vessel speeds will not increase for safety and to limit impacts on adjacent features..

The six model conditions (EC, FWOP, FWPFB, ALT1, ALT2, and ALT3 and associated vessel input parameters shown in Table 4-1) were each run on the south, central, and north meshes described in Section 4.3, totaling 18 model simulations (6 channel conditions on 3 meshes). Five additional simulations and comparisons were made for FWOP and the four FWP conditions (FWPFB, ALT1, ALT2, ALT3) with additional future projections of sea level change adding 1.43 m to the initial condition on the central mesh. The RSLC runs focused on the central mesh as it was the largest and covered the greatest length of the channel. The intent is to make relative comparisons between the FWOP and the FWP conditions with and without sea level change and extrapolate those findings to the other meshes. The 1.43 m value used for RSLC scenarios was calculated using the standard USACE method as described in the following subsection.

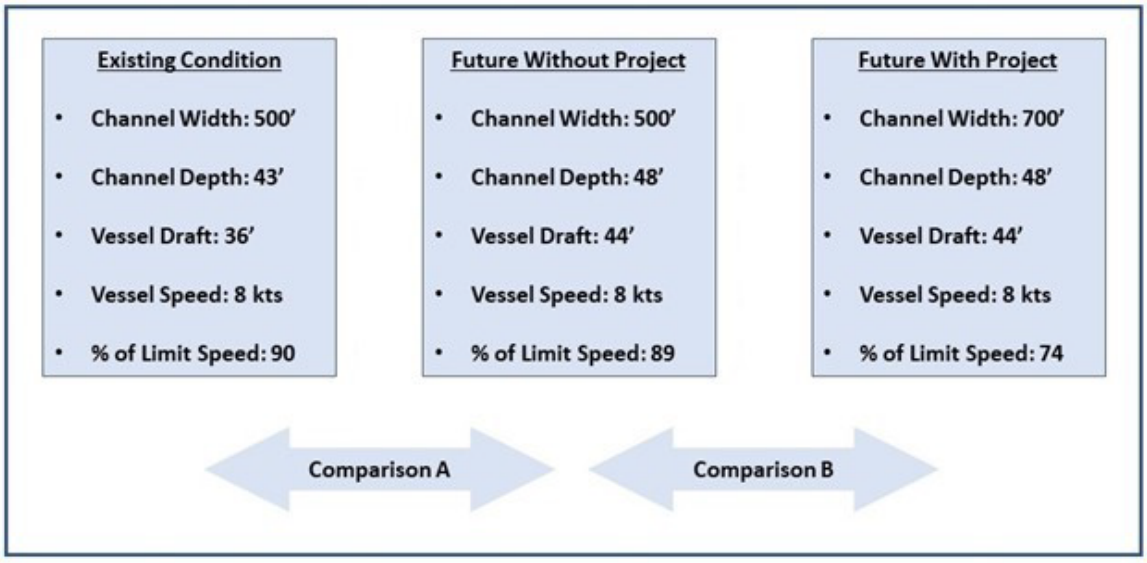

Figure 4-5
Scenarios Modeled: Vessel Size, Draft and Speed for Each Channel Configuration

The channel widths and depths in Figure 4-5 are representative of an idealized channel cross-section in for the reaches between Sabine Pass Channel and Port Arthur Canal. The 43 ft channel depth for the EC presented is larger than the authorized depth, but matches the observed bathymetry and was selected to be consistent with the previous analysis at the "south site" evaluated in Maynord (2003) and USACE (2008) as part of the SNWW CIP. Therefore, the percent limit speeds presented in Table 4-1 and Figure 4-5 will be higher in the narrower (400 ft) sections of the EC channel and are considered conservative. Comparisons to the AIS values indicate the vessels are transiting faster than predicted by the Schijf equations. This is explained by the theoretical blockage ratio (vessel cross-section over channel cross section) being larger than the prototype. The idealized channel considered does not account for additional flow area outside of the navigation channel nor does it account for the vessel cross-sections designed to be more hydrodynamically efficient.

4.6.3 Limiting Speed

The Schijf equation is used to estimate the drawdown and return current for a vessel transiting a confined or restricted channel (Schijf and Jansen 1953). The theory is derived by solving the system of Bernoulli and continuity equations (1) and (2) at two channel cross-sections, one in the undisturbed water ahead of the vessel and a second at mid length of the vessel (Huval 1980).

$$z = \frac{(V+U)^2 - V^2}{2g} \tag{1}$$

$$VA_c = (V+U)A_w \tag{2}$$

Where,

$z =$ drawdown

$V =$ vessel velocity

$U =$ return current

$g =$ acceleration of gravity

$A_c =$ undisturbed channel cross-sectional area ahead of the vessel

$A_w =$ cross-sectional area of the channel at mid length of the vessel not including the submerged vessel area.

These relationships can also be used to calculate a theoretical maximum speed a self-propelled vessel can achieve in a restricted channel (Schijf and Jansen 1953) known as the "limiting speed." The actual maximum speed is determined by the vessel pilot based on safety and other factors. The theoretical limiting speed occurs when the Froude number is one and the flow is critical.

$$Fr = \frac{(V+U)}{\sqrt{g\bar{d}}} \tag{3}$$

Where,

$\bar{d} =$ mean depth is (A_w/W) and W is the channel width at the daylight line. A schematic of the parameters in these equations are shown in Figure 4-6.

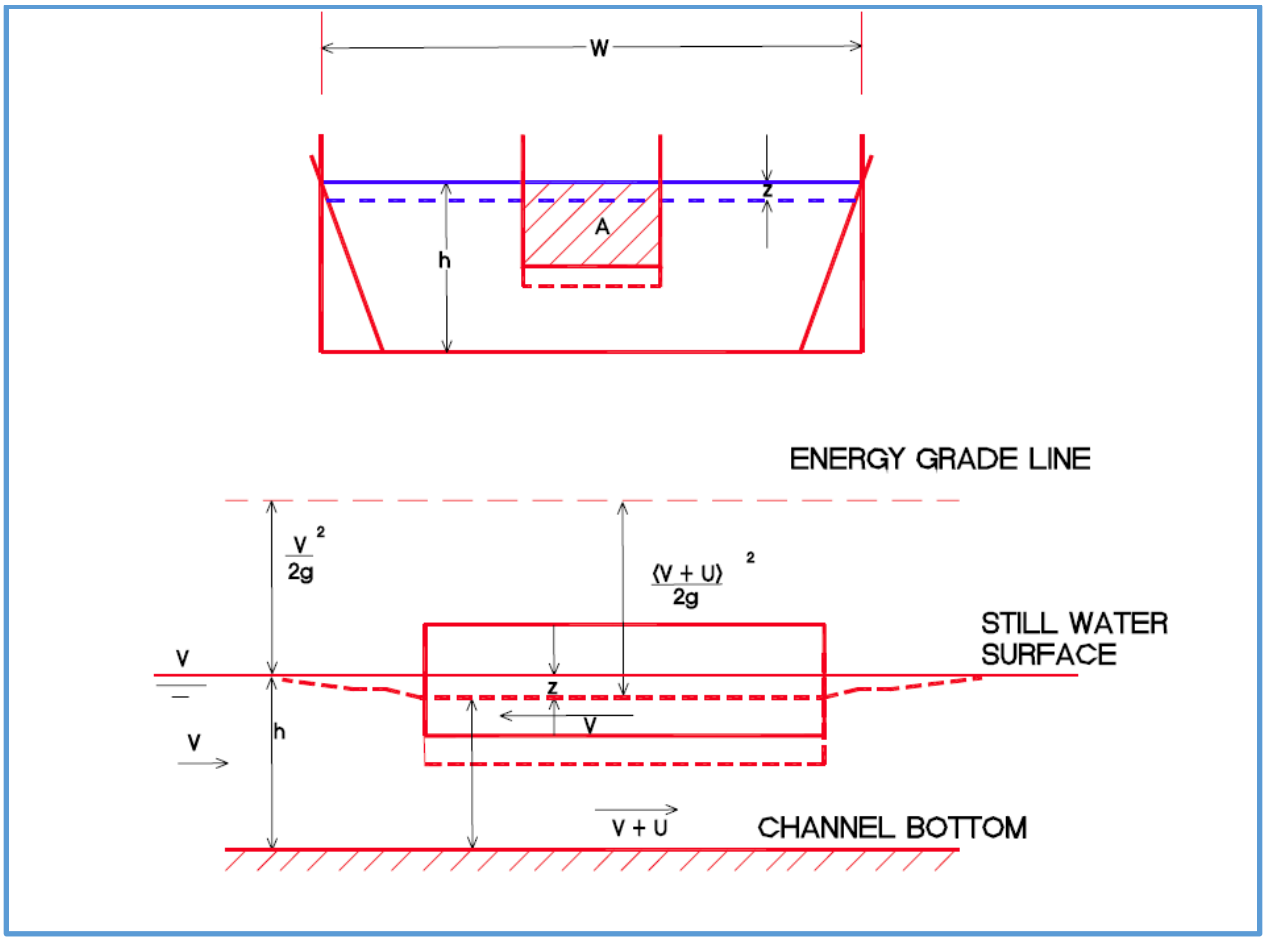

Figure 4-6
Example Schematic for the Schijf Equations

An explicit formulation for the limiting speed is given as (Huval 1980):

$$\frac{V_L}{\sqrt{g\bar{d}}} = \sqrt{8\cos^3\left(\frac{\pi}{3} + \frac{\cos^{-1}}{3}\left(1 - \frac{1}{B_R}\right)\right)} \quad (3)$$

Where,

B_r = is the blockage ratio defined as A_w/a and a is the statically submerged vessel cross-section area.

The actual speed of a vessel in a restricted channel will not exceed 80 to 90 percent of the Schijf limiting speed (Jansen and Schijf, 1954). As the vessel speed reaches this range, fuel economy drops sharply, so pilots generally will not exceed this range to conserve fuel. This modeling effort started with the vessel parameters for the FWOP condition, determined the limited speed, which is 89 percent, and then chose the vessel parameters for the other channel configurations such that the vessel was traveling at approximately the percentage of the limiting speed. For the EC model the vessel draft was reduced to achieve approximately 90 percent of the limiting speed. The

reduced draft was also necessary because the channel depth was shallower. For one of the FWPFB models, the vessel speed was increased to maintain the limiting speed when the channel cross-section was enlarged through the widening. The FWPFB condition was also run with the same vessel speed as the FWOP (8 kts) for direct comparison.

As an example, for the FWOP condition the limit speed was calculated to be 15.1 ft/s (or 8.95 kts) as shown in equation 4 below. The selected speed of 8 kts is 89 percent of the 8.95 kts limiting speed.

$$\frac{15.1}{\sqrt{(32.2)(41.34)}} = \sqrt{8\,cos^3\left(\frac{\pi}{3} + \frac{cos^{-1}}{3}\left(1 - \frac{1}{3.97}\right)\right)} \quad (4)$$

4.6.4 Relative Sea Level Change

Analysis of relative sea level change (RSLC) was incorporated into the SNWW hydrodynamic modeling in accordance with USACE guidance contained in ER 1100-2-8162 "Incorporating Sea Level Change in Civil Works Programs." ER 1100-2-8162 provides a method (or methods) for determining the range of possible future rates of global, regional, and local RSLC that planning studies are required to consider. The RSLC rates represent eustatic sea level change and vertical land motion, and are classified as "low," "intermediate," or "high" scenarios, as follows:

- The low rate is based on linear trends developed from historical observed data from tide stations.
- The intermediate rate is determined based on the modified NRC Curve I (NRC 1987).
- The high rate is determined based on the modified NRC Curve III (NRC 1987).

The low, intermediate, and high RSLC scenarios for this study are based on NOAA 8770570 Sabine Pass North, TX located near the entrance the Gulf of Mexico to the SNWW. Scenarios for RSLC rates for 20, 50 and 100 years were generated using USACE's online sea-level calculator (https://cwbi-app.sec.usace.army.mil/rccslc/slcc_calc.html) based on start of the SNWW CIP construction in 2020 and a 50-year period of analysis for the channel widening starting in 2025. Values for the RSLC scenarios are given in Table 4-2, and curves for 2020 to 2075 are shown in Figure 4-7.

Table 4-2: RSLC Values Developed from USACE's Online Sea-Level Calculator at NOAA 8770570.

Scenario	2020-2045	2020-2075	2020-2125
Low	0.14 m (0.46 ft)	0.31 m (1.02 ft)	0.59 m (1.95 ft)
Intermediate	0.20 m (0.64 ft)	0.48 m (1.56 ft)	1.05 m (3.45 ft)
High	0.37 m (1.22 ft)	1.00 m (3.29 ft)	2.51 m (8.22 ft)

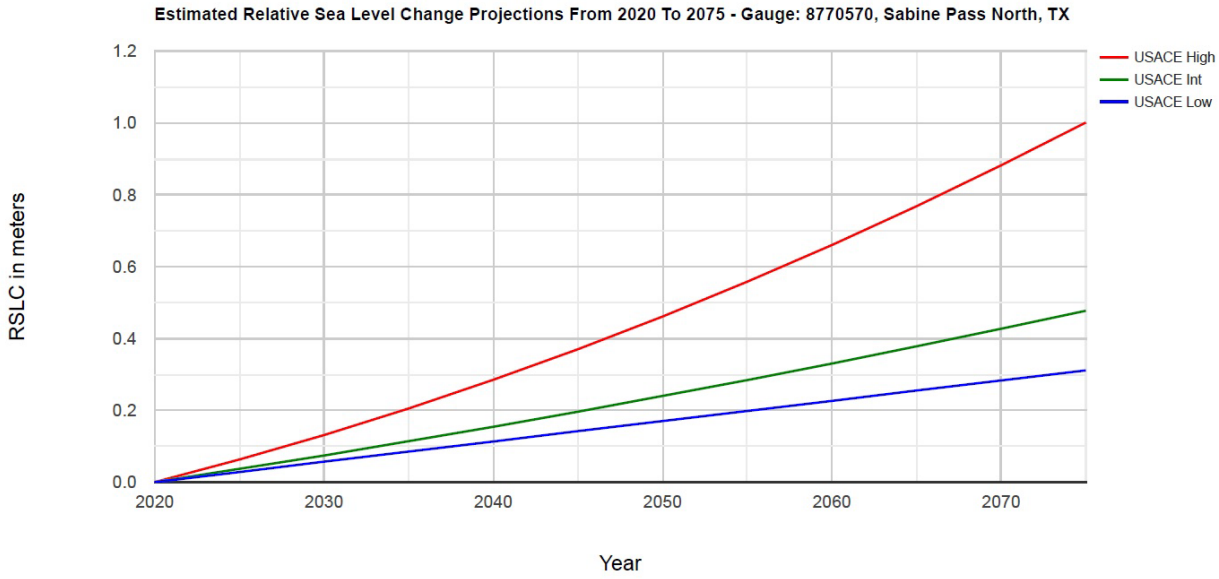

Figure 4-7
RSLC Curves Based on USACE Sea-Level Calculator at NOAA 8770570: 2020 to 2075

The low RSLC rate, based on the observed data at NOAA 8770570, is approximately 5.66 mm/yr and gives 0.31 m RSLC over the period of analysis of the SNWW plan alternatives. The intermediate and high RSLC scenarios show accelerating RSLC and result in 0.48 m and 1.00 m, respectively, at the end of the analysis period. The low, medium, and high RSLC scenarios are calculated with respect to the +0.43 m NAVD88 to the approximate 2020 mean sea level, as such, the totals are +0.74 m, +0.91 m and +1.43 m NAVD88 respectively. The ER 1100-2-8162 guidance suggests a single scenario can be used to identify the preferred alternative under that scenario. The preferred alternative's performance can then be evaluated under all RSLC scenarios to determine its overall performance. This approach is appropriate when project performance is not highly sensitive to RSLC. For this analysis, the high scenario for the 50-year RSLC is used within the hydrodynamic modeling. The high scenario was applied to blanket possible RSLC effects that could then be used to infer project performance for other scenarios.

5 Model Calibration and Validation

5.1 Wave Data Field Investigation

In support of the modeling work, HDR conducted a field investigation on August 19 and 20, 2020. The purpose of the field investigation was to gather drawdown and return current data for calibration and validation of the numerical modeling. Acoustic Doppler Velocimeters (ADVs) were deployed to measure water levels and currents at several locations adjacent to the channel in approximately 2.5 m (8 ft) water depth. During the field deployment, a total of four transiting vessels were observed from which the field team was able to collect six different vessel wake events. The datasets consist of three outbound vessels at a single location on August 19, 2020 and an inbound vessel at three separate locations on August 20, 2020. Vessel parameters such as

direction, length overall (LOA), breadth, draft, and speed were gathered from MarineTraffic.com; a webservice that provides access to the automatic identification system (AIS) real-time ship tracking. A summary of the observed vessels and their dimensions is presented in Table 5-1. Of the six events from the four vessels, two datasets from the largest vessels were chosen for calibration and validation.

Table 5-1
Vessel Traffic Direction, Dimensions, and Draft During Field Investigation

Vessel Specs	Vessel			
	BW Kizoku	Sulphur Enterprise[1]	Nave Orbit[1]	Star Luster
Model Use	Validation	Not Presented	Not Presented	Calibration
Class	Aframax	MRT or Coastal Tanker	Panamax	MRT or Panamax
Date	08/19/2020	08/19/2020	08/19/2020	08/20/2020
Direction	Outbound	Outbound	Outbound	Inbound
Speed	6-8 kts	6-8 kts	6-8 kts	8-12 kts
LOA	230 m (755 ft)	160 m (524 ft)	183 m (600 ft)	205 m (671 ft)
Breadth	37 m (121 ft)	27.4 m (90 ft)	32.2 m (106 ft)	32.3 m (106 ft)
Draft	11.6 m (38 ft)	10.7 m (35 ft)	10.9 m (36 ft)	8.1 m (27 ft)
ADV Location	2	2	2	4, 5, 6

[1]The measured wakes from the Sulphur Enterprise and Nave Orbit were smaller (~ 1 ft) than the other vessels because of the smaller vessel sizes and therefore were not modeled for the validation.

The Star Luster observations at ADV 2 were chosen as the calibration dataset. These observations featured the largest measured drawdown and return current and occurred at a narrow section of the channel. The BW Kizoku observations at ADV 5 were chosen as the validation dataset, where the channel is wider. The vessel speed from the AIS data in the vicinity of ADV locations 2 and 5 was not constant. For example, the speed at several locations near the ADVs are shown on the maps in Figure 5-3 and Figure 5-6. The red dots indicate the location of the reported AIS vessel speed which is annotated on the dot. The modeling applied a constant vessel speed for each run, and several different runs with different speeds were performed during the calibration. The vessel speeds were selected to bracket the range of speeds observed by the AIS data.

The ADV instruments recorded water levels and velocity at 8 hertz (Hz) resolving both the low and high frequency vessel wakes. Prior to comparisons with the AdH model, a low-pass filter of a 5-second window length was applied to isolate the lower frequency waves the model is intended to capture. The water level data collected and used in the model validation are given in Figure 5-1 and Figure 5-2 representing the BW Kizoku and the Nave Orbit, respectively. The figures show the raw measured data and the filtered data overlaid on the same graph in the top panels and the difference between the raw and filtered data in the lower panels. Both figures show a clear drawdown on the order of 2 minutes in duration followed by shorter period waves. The filtered

data does well to capture the longer period drawdown, which is what AdH is able to simulate, but removes the shorter period stern waves that will be evaluated using Maynord's (2003) empirical equations because the model is not suitable for capturing.

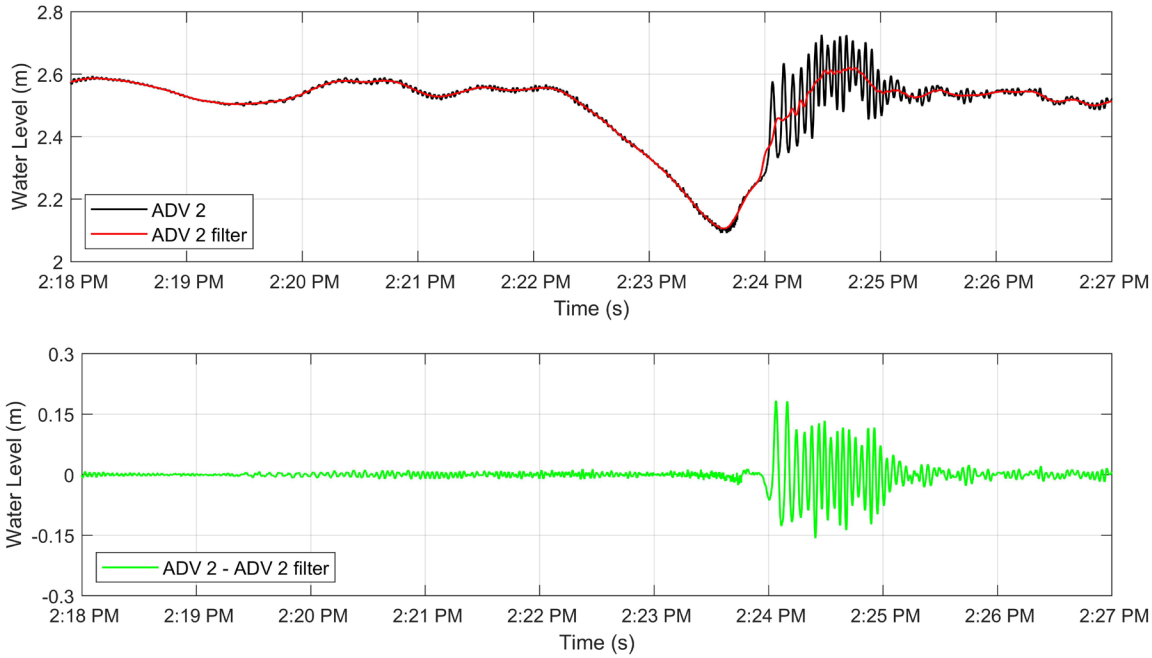

Figure 5-1
Water levels measurements from ADV 2 on October 19, 2020 (BW Kizoku Wake)

Top panel shows raw data (black line) and data filtered with a 5-second moving average (red line). Bottom panel shows only the high frequency data obtained by subtracting the filtered data from the raw data.

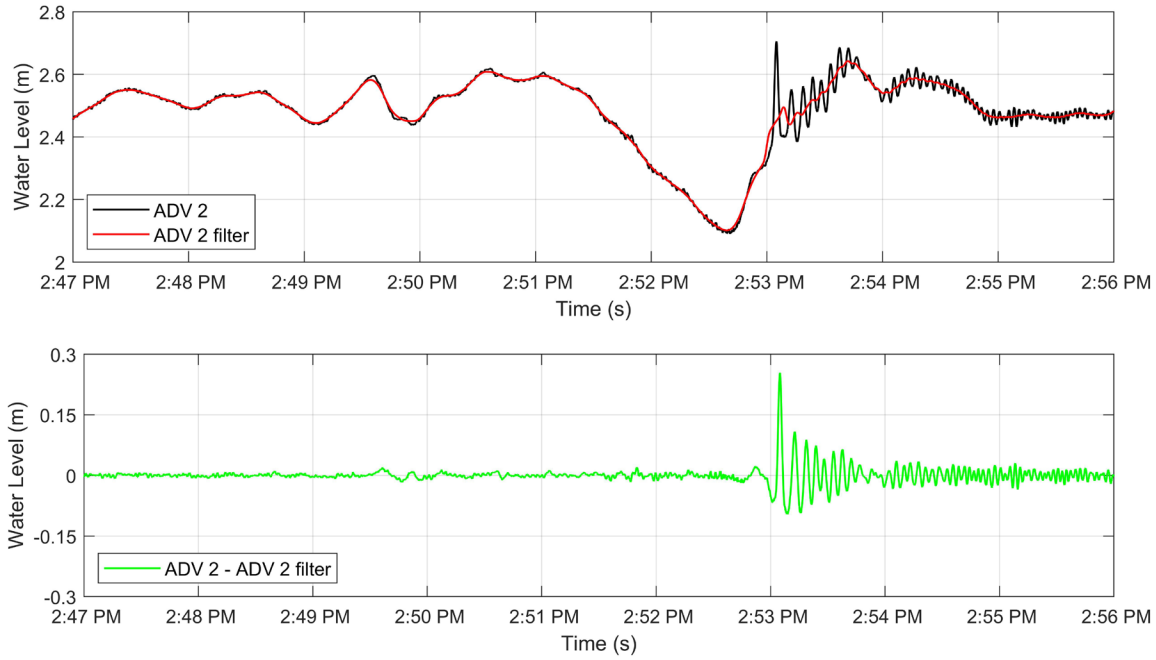

Figure 5-2
Water levels measurements from ADV 2 on October 19, 2020 (Nave Orbit Wake)

Top panel shows raw data (black line) and data filtered with a 5-second moving average (red line). Bottom panel shows only the high frequency data obtained by subtracting the filtered data from the raw data.

5.2 Model Calibration

The model calibration was run for the Star Luster dataset focusing on the event that had the greatest hydrodynamic effects (TSW and return current). The model used the central mesh discussed in Section 4.3, but updated the mesh resolution along the sailing path to correspond to the vessel being modeled. Initially model runs were made using the vessel parameters determined from previous ADH modeling on the Texas Coast which are shown in Section 4.4. All model runs were performed with a constant vessel speed (i.e., not varying within a given model run). Multiple vessel speeds were modeled in the calibration and validation runs to bracket the speeds observed on MarineTraffic.com since the vessels were varying speed. The speed at several locations near the ADV 5 deployment location are shown on the maps in Figure 5-3. Measured and modeled water surface elevation and current speed plots are shown in Figure 5-4. For the calibration effort vessel speeds of 10 kts, 10.5 kts, and 11 kts were modeled.

Figure 5-3
Vessel Star Luster Speed (kts) and Position Data from AIS Relative to ADV 5 Field Measurement Location (vessel traveling inbound)

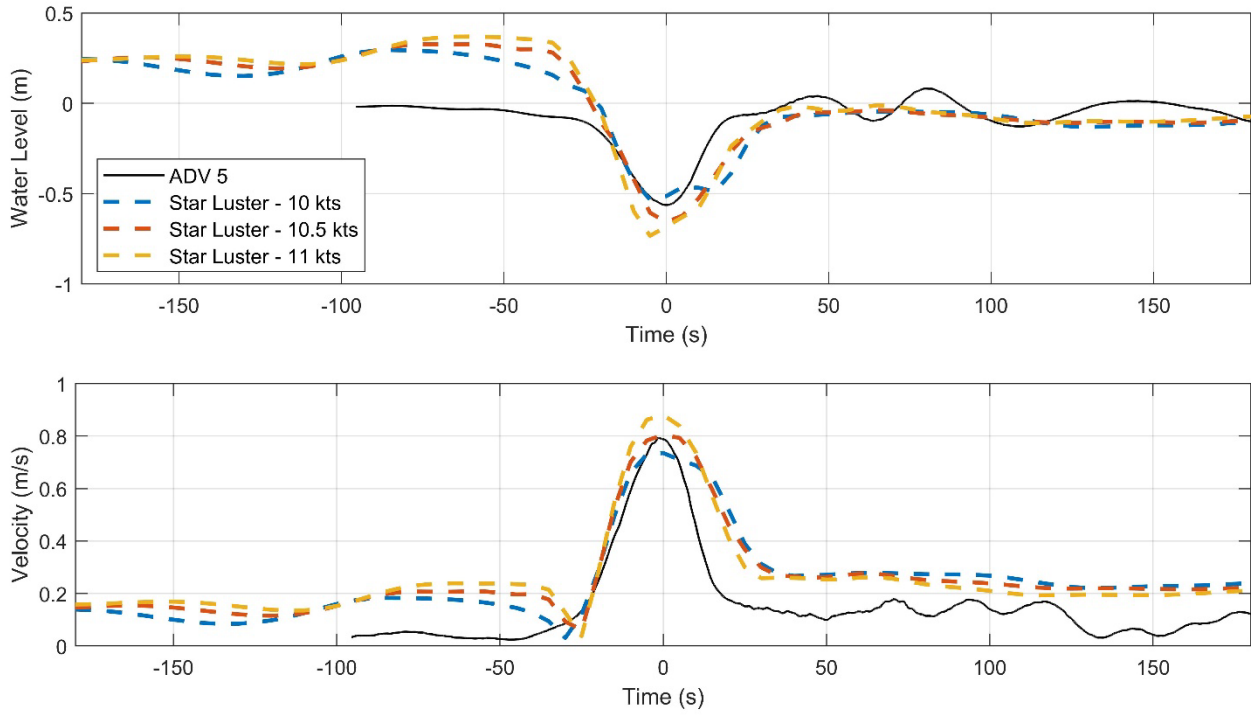

Figure 5-4
Water Surface Elevation and Velocity Comparisons of ADV 5 Observations and AdH Model Results for Vessel Star Luster

The comparisons between the observed and modeled water level and velocity time series for the Star Luster vessel, recorded at ADV Location 5, are shown in Figure 5-4. For the water level plot,

the modeled water level is presented relative to the initial model water level (e.g., the still water level is represented by 0 m in the figure). Note the water level for the model runs in the figure is approximately +0.25 m because the model creates a large bow wake that propagates down the confined channel, but the water level returns to 0.0 m beyond the extent shown in the figure in the both the positive and negative time direction. This bow wake has been observed in previous AdH modeling of vessels and the model was still found to reproduce the drawdown and water velocity. The drawdown in the model is measured relative to the initial model water level, or 0.0 m in the figure. The observed water level at ADV 5 was translated based on the average water level when removing the vessel passing so that 0 m the model and measured data can be compared directly.

From the figure, the drawdown in the model performs well to predict the total drawdown within approximately 0.15 m of the observed dataset, depending which modeled vessel speed is evaluated. As stated prior, the model drawdown is measured from 0.0 m (the initial water level in the model). The velocity comparison also agrees within approximately 0.0 to 0.08 m/s depending which modeled vessel speed is considered. The model results showed the minimum water level and maximum velocity occur at the same time, which suggests these minimum water level and maximum velocity values correspond to the drawdown and return current introduced in Section 1.2 and presented theoretically in Section 4.5. The 10.5 kts vessel speed best matches both the water level (drawdown) and velocity (return current) and was chosen for the subsequent calibration sensitivity testing discussed in the remainder of this section.

A calibration was performed to test the influence of the Manning's n value on model results. The n values tested were 0.15, 0.20, 0.25 and 0.30. The Manning's n value had minimal effect on the model results with the maximum drawdown varying 0.05 m and the maximum return current varying 0.01 m/s. Time series of modeled water level and velocity for all four manning's values are shown in Figure 5-5 along with the measured data from ADV 5. The n=0.2 Manning's value has been used in previous Texas Coast ADH modeling efforts performed by HDR and was selected and used throughout the remainder of the modeling. Model error is discussed in Section 5.4.

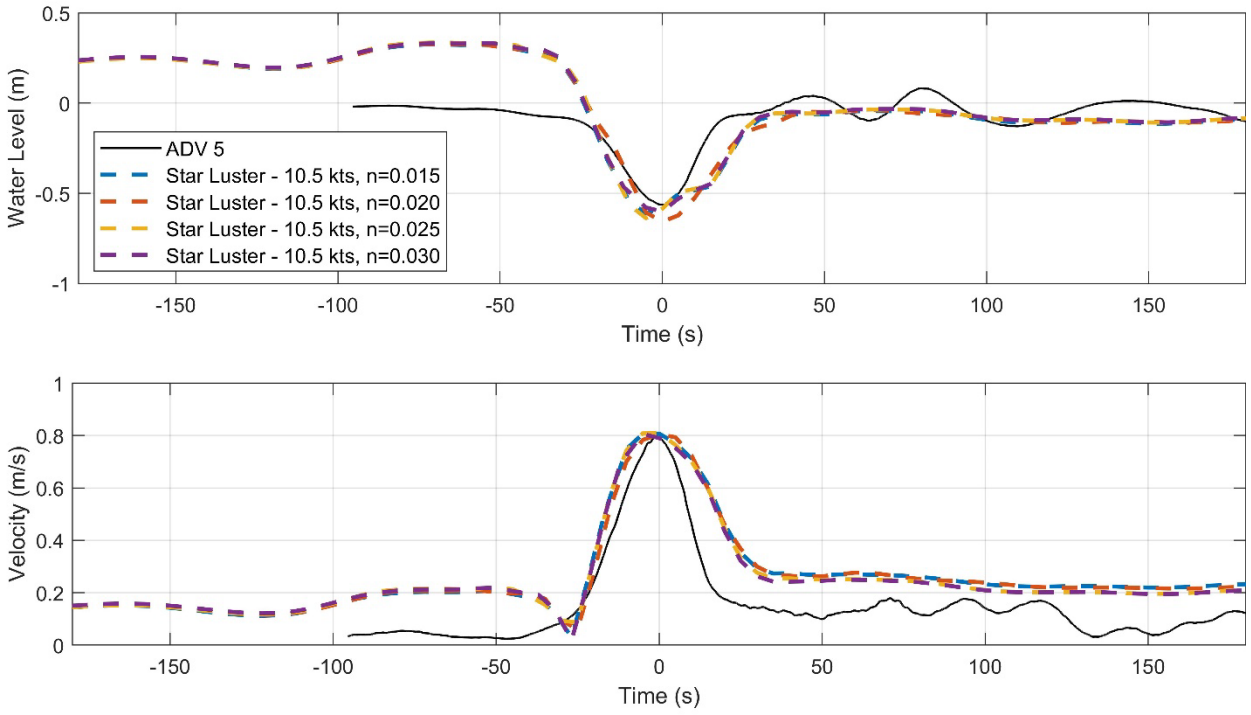

Figure 5-5
Water Surface Elevation and Velocity Comparisons of ADV 5 Observations and AdH Model Results for Vessel Star Luster

5.3 Model Validation

The BW Kizoku vessel with the second largest observed hydrodynamic effects was used for model validation. The vessel speed at several locations near the ADV 2 is shown on the maps in Figure 5-6. Speeds of 7 kts and 8 kts were modeled to represent the BW Kizoku speed as it approached ADV 2 from the north. There was an approximately 0.5 kts current towards the north (not shown) during the time of the BW Kizoku transit, therefore the vessels speed over water was approximately 0.5 kts faster than the speed over ground shown in Figure 4-4. Comparisons between the observed and modeled water level and velocity time series for the BW Kizoku vessel, recorded at ADV Location 2, are shown in Figure 5-7. In these comparisons, the observed 0.35 m drawdown was underpredicted by AdH by approximately 0.20 to 0.25 m, depending on modeled vessel speed. The modeled velocity also underpredicted the observations, with the 7 kts model vessel speed underpredicting by 0.40 m/s and the 8 kts model vessel speed by 0.25 m/s. The BW Kizoku was the largest vessel observed (Table 5-1) and is an Aframax class which is most similar to the Suezmax vessel used for production runs.

Figure 5-6
Vessel BW Kizoku Speed (kts) and Position Data From AIS Relative to ADV 2 Field Measurement Location

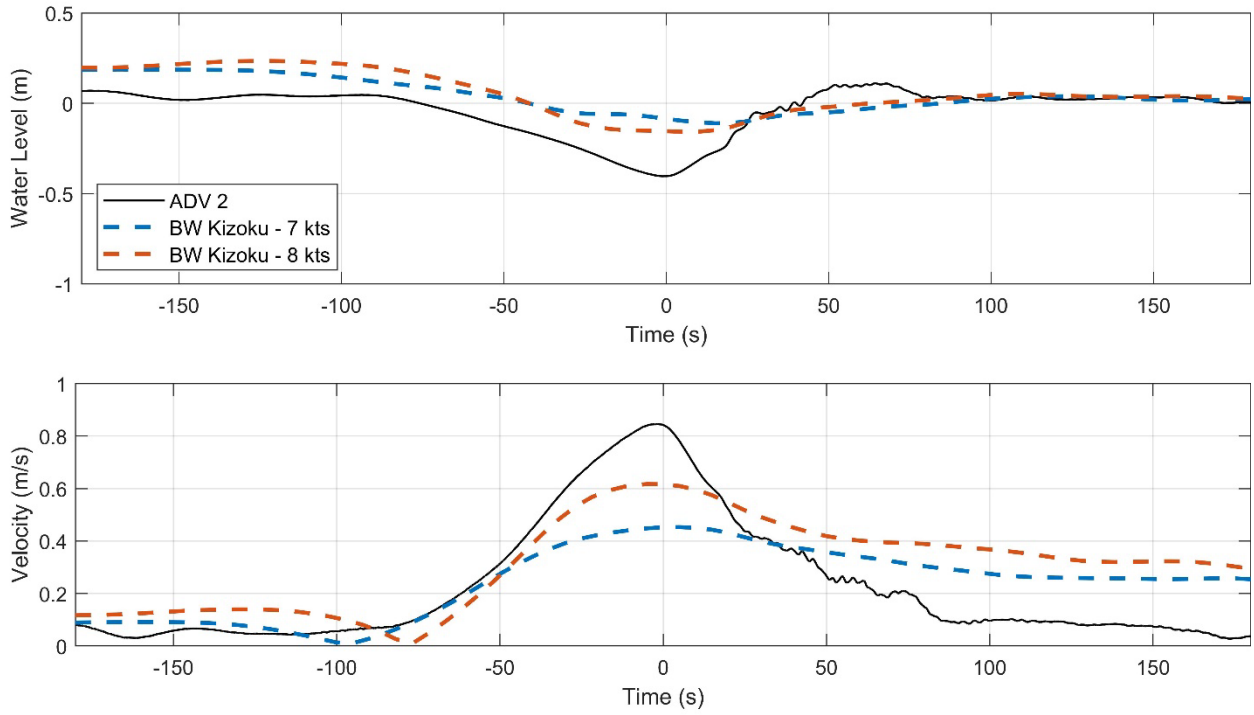

Figure 5-7
Water Surface Elevation and Velocity Comparisons of ADV 2 Observations and AdH Model Results for Vessel BW Kizoku

Additional examination of the modeling parameters and results was performed to better understand the cause of the model underprediction for the BW Kizoku at ADV 2. One observation was that field staff deployed ADV 2 in approximately 2.5 m water depth, but the water depth in the model mesh was approximately 4 m at this location, indicating the model elevation data may not be consistent with the actual bathymetry at the time of the field data collection in this area. As an initial investigation, the model results for drawdown and return current were reviewed for spatial variability in the vicinity of ADV 2 to see if the model better predicts the peak drawdown and return current in the vicinity of modeled ADV2 location. These results for peak drawdown and peak velocity are shown in Figure 5-8 and Figure 5-9, respectively. The peak drawdowns from the validation model both north and south of ADV 2 site are much closer to the 0.4 m drawdown observed. Similarly, Figure 5-9 shows peak return current also increased in the narrower sections of channel where they better matched the 0.85 m/s observed return current from the BW Kizoku. In both Figure 5-8 and Figure 5-9, the location of ADV 5, where data were collected the following day for the Star Luster vessel, is given for reference.

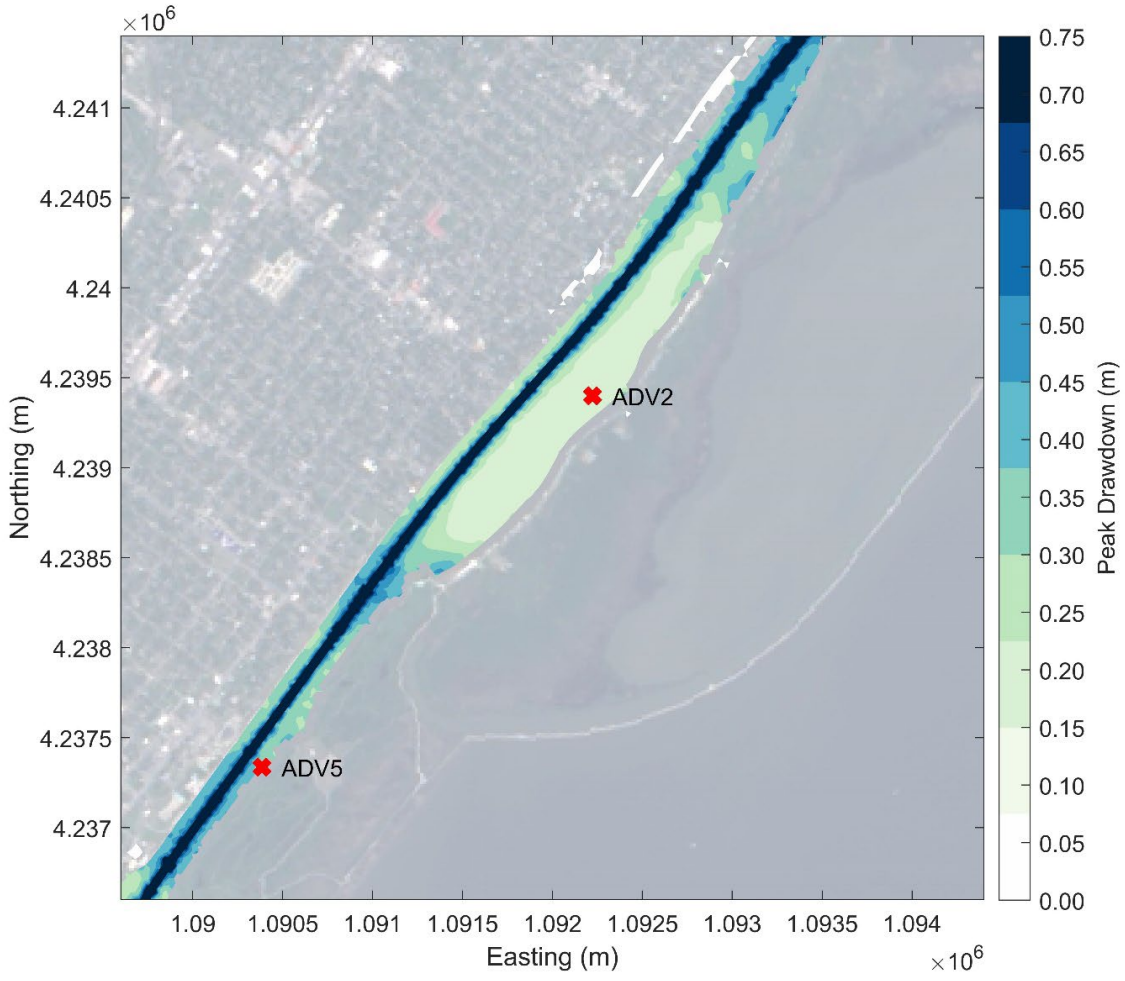

Figure 5-8
Spatial variation of peak drawdown (m) from calibration vessel BW Kizoku (8 kts)

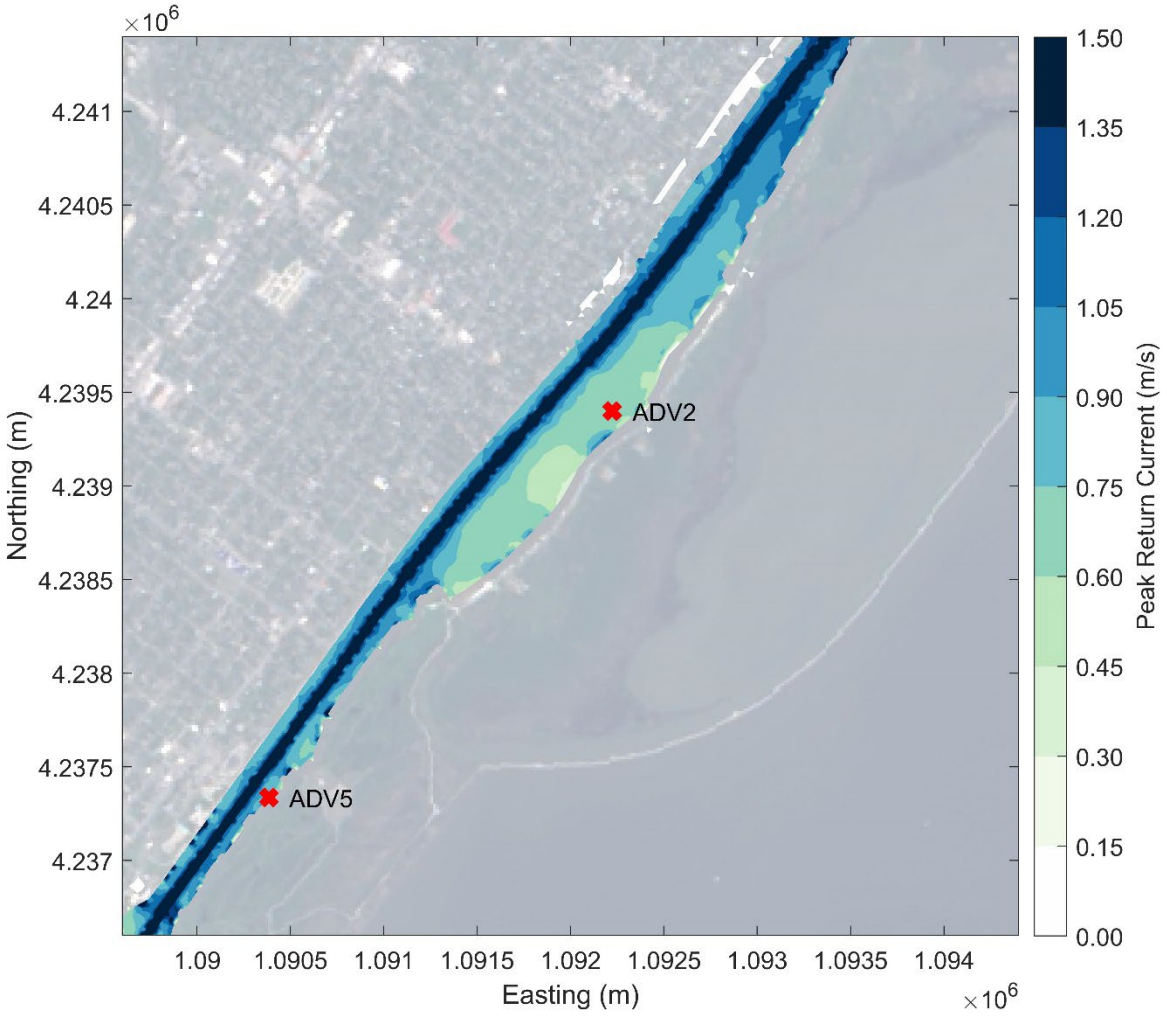

Figure 5-9
Spatial variation of peak return current from calibration vessel BW Kizoku (8 kts)

As shown in Figure 5-8 and Figure 5-9, the modeled hydrodynamics are more energetic in the narrower sections of the channel north and south of ADV 2 indicating the model is predicting the same magnitude of hydrodynamic response as observed in locations close to the ADV.

The modeled bathymetry for this section of the channel was likely deeper than actual for the submerged shelf between the channel and the bank based on the field observations. The field observations measured at ADV Location 2 were located on the eastern (Red) side of the waterway approximately even with station 93+750. This location is a narrow section of the navigation channel (400 ft); however, there is a wide submerged shelf to the east between the channel and the bank. It was noted in the field that this shelf was relatively shallow (approximately 2 to 5 m based on field engineers' lead line soundings) and extended well away from the bank towards the channel. However, it was identified after the fieldwork that the model bathymetry is approximately 8 m in this area, which is significantly deeper. Transiting vessel hydrodynamics increase in magnitude as the waterway is constricted. The difference in waterway constriction is a possible explanation in the variance of the measured and modeled hydrodynamics at this location.

An additional dataset for depths around ADV 2 became available with a new version of NOAA CUDEM data in May 2021. The bottom elevations in the section of SNWW near ADV 2 were compared between the bathymetry data used in the mesh development (an earlier version of the CUDEM data) and the updated bathymetry dataset from May 2021. The comparison, shown in Figure 5-10, shows the area to be shallower than the previous modeled version of the CUDEM data by up to 2.5 m. This elevation change between dataset versions supports the earlier conclusion that the model underprediction at ADV 2 was an artifact of the modeled depths being too deep, resulting in a larger channel cross-sectional area than existed at the time of the ADV field measurements which theoretically would reduce the hydrodynamic response in the model. Therefore, an initial validation run was performed using the new CUDEM dataset for elevation to check this theory. The results are shown in Figure 5-11.

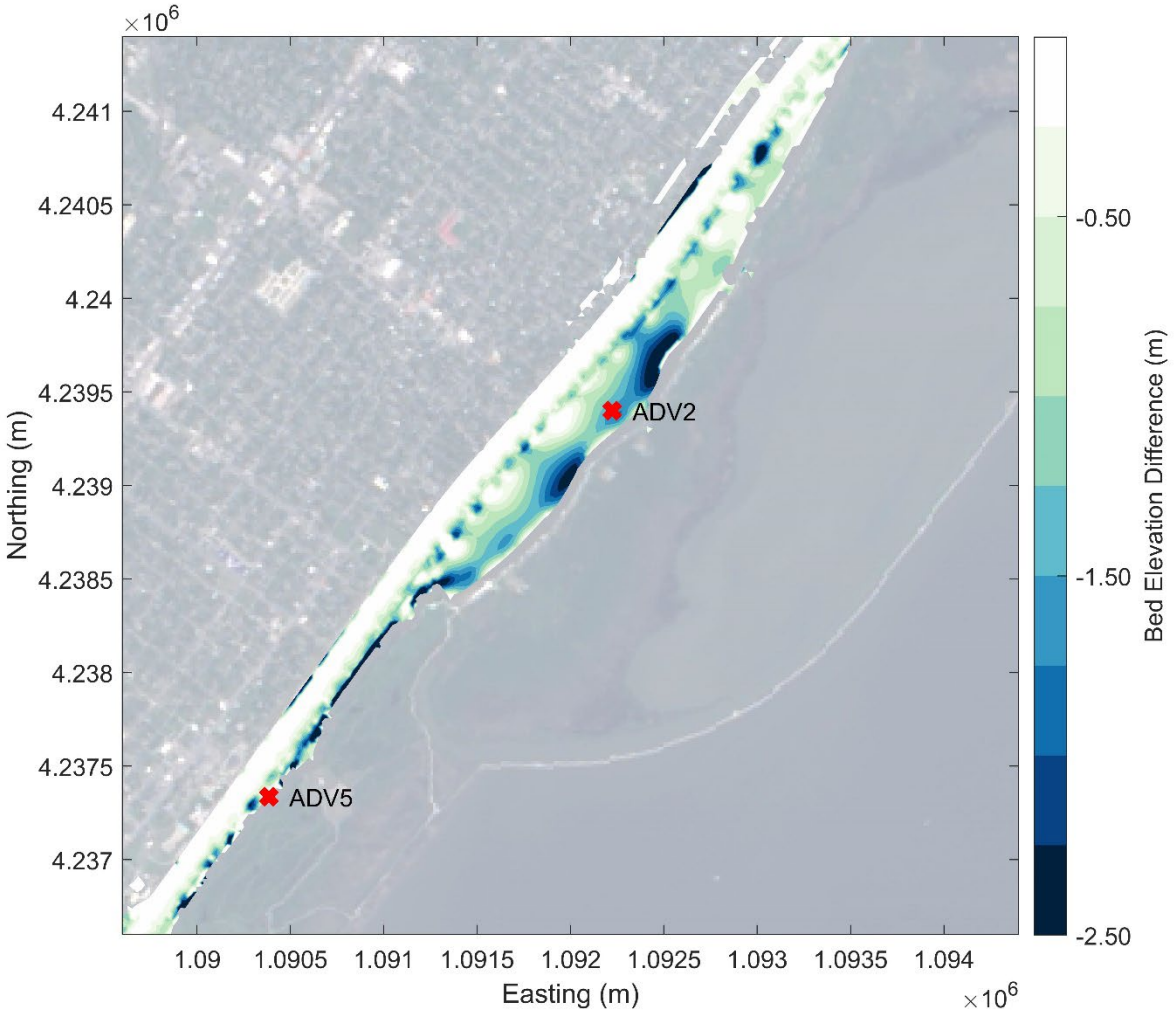

Figure 5-10
Elevation change between original CUDEM used for modeling and the newly released May 2021 CUDEM for the area surrounding ADV 2
(Negative values indicate a higher bottom elevation (shallower water) in the more recent data set.

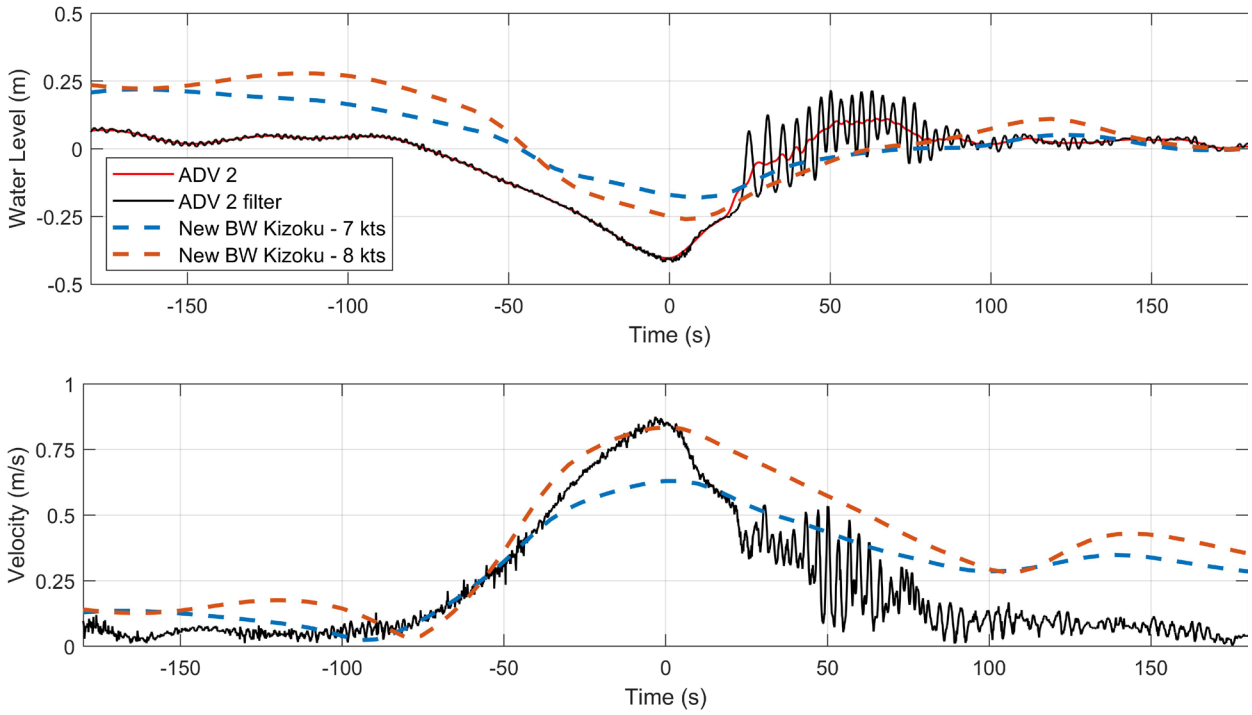

Figure 5-11
Water Surface Elevation and Velocity Comparisons of ADV 2 Observations and AdH Model Results for Vessel BW Kizoku using updated CUDEM elevation dataset for mesh development

Figure 5-11 shows improvement in the model validation with the 8 knots modeled vessel speed underpredicting the drawdown by approximately 0.1 m where the previous validation run underpredicted the drawdown by nearly 0.2 m. The peak velocity comparison in Figure 5-11 shows the 8 knots vessel speed nearly matching the observed peak velocity where the previous model run underpredicted by approximately 0.25 m/s. These results showed improvements over the original model run using the old CUDEM dataset, but the bottom elevations in the dataset still appeared deeper than observed in the field. Differences between a Digital Elevation Model and measured elevation data are inherent and expected and represent part of the potential model error. However, the model purpose is to compare the vessel effects between several channel alternatives (base-to-plan testing), all of which will use the same base elevation dataset thus eliminating some of the structural uncertainty in the model. Because the May 2021 CUDEM dataset was not available at the time the modeling was performed, and the model comparisons will use the same base elevation dataset, the production model runs discussed in the remainder of the report were not rerun with the updated CUDEM dataset.

5.4 Model Error

Model error is important for understanding the model's ability to accurately recreate the hydrodynamics from a passing vessel event. The mean absolute error was used to assess model error. The mean absolute error is defined as:

$$\text{Error}_{\text{model, drawdown}} = \frac{\sum |Drawdown_{\text{max: model}} - Drawdown_{\text{max: meas}}|}{N}$$

$$\text{Error}_{\text{model, current speed}} = \frac{\sum |Current\ Speed_{\text{max: model}} - Current\ Speed_{\text{max: meas}}|}{N}$$

It is preferable to calculate the mean absolute error based on a large number of data points (N in the equation). In this report and analysis, the model comparisons and conclusions focused on peak drawdown and peak current speed as defined in the above equations, but as presented in Section 5.1 only two observations were considered reasonable for modeling and model error calculation. Further one of the data points is expected to have some model error because of the model bathymetry not matching the field observations as discussed in the previous section. Noting the limitations with the model error calculation, the calculated values are shown in Table 5-2.

Table 5-2
Model Mean Absolute Error

Parameter	Model Mean Absolute Error
Peak Drawdown (m)	0.15
Peak Return Current (m/s)	0.10

These model errors should be considered when reviewing the model results, but the limited data points for error calculation and the expected model results skew due to bathymetry differences should also be considered. Therefore, the model error (and associated model uncertainty) is discussed in the text in the results, but not shown on the figures or tables. The primary purpose of the model is to understand the differences between the without and with project conditions, which the model is still expected to capture.

6 Results and Discussion

The results of the modeled vessel-induced water levels and velocities for the channel configurations are compared using three analyses. The first analysis compares modeled water level and velocity time series near the bank at several representative locations adjacent to the proposed project areas. Minimum water levels (drawdown) and maximum velocities (return current) from the time series are then tabulated and differences between alternatives are computed. In addition to the time series plots, this analysis includes a set of side-by-side results of model elevation, water level, and velocity corresponding to the time of the peak drawdown and return current at one of the save points. The second analysis compares modeled results within the navigation channel along the entire reach from Sabine Pass to Beaumont. Rather than presenting time series, these comparisons consider channel averaged peak drawdown and return current which is analogous to the Schijf equations U and z from section 4.5. These two analyses are discussed in terms of comparisons A and B introduced in Section 4.5 and shown in Figure 4-5. These comparisons are repeated on the RSLC scenarios for FWOP and FWP conditions and presented in Sections 6.3 and 6.4. The third analysis used an empirical methodology developed by Maynord (2003) to compute and compare the surge portion of the full TSW, or the portion of the vessel response that extends above the initial water level and is not captured by the numerical model, for the various project

alternatives. This third analysis approach is consistent with Maynord (2003), where the full TSW is comprised of the drawdown (numerical model) and the surge (empirical).

A significant consideration in these results is the vessel speed. Although the channel cross-section would be increasing and therefore the theoretical maximum vessel speed or limiting speed (see Section 4.5), the results presented here are based on an equal vessel speed between FWOP and all widening channel configurations. This is based on communications with the SNND Pilots that vessel speeds will not increase for safety and to limit impacts on adjacent features. Modeling was performed for a faster vessel speed in the widened channel but is not presented here based on these discussions. Although portions of the channel would be widened and therefore could support a faster vessel speed, these areas would be limited and not representative of the entire channel length.

6.1 Analysis 1: Water Level and Velocity Time-Series Near Channel Bank

Model results at 10 save point locations along the SNWW were extracted from each of the channel configuration models for the Suezmax vessel. A map of the save point locations is shown in Figure 6-1. Save points were chosen at locations within the channel improvement areas to provide insight regarding potential changes to bank erosion forces associated with the proposed project conditions. The save point locations were selected to lay on the 3.5 m depth contour (relative to initial still water level in the model) between the channel and the bank. If the 3.5 m depth contour changed because of the FWPFB, ALT1, ALT2, or ALT3 channel widening, the save point location was translated towards the bank accordingly. Extracted time series were evaluated at each of the save points and representative time series at the below locations are shown in this report.

- 50+000 located in the Port Arthur Canal (Figure 6-2)
- 85+000 located in the Sabine-Neches Canal North (Figure 6-4)

Location 85+000 is approximately the same location as ADV 5 where the Star Luster Aframax vessel was measured as part of the calibration. Locations 50+000 and 85+000 are also approximately the same locations as the “South” and “North” sites analyzed in Maynord (2003). The remaining save point locations are summarized in Table 6-1 through Table 6-4.

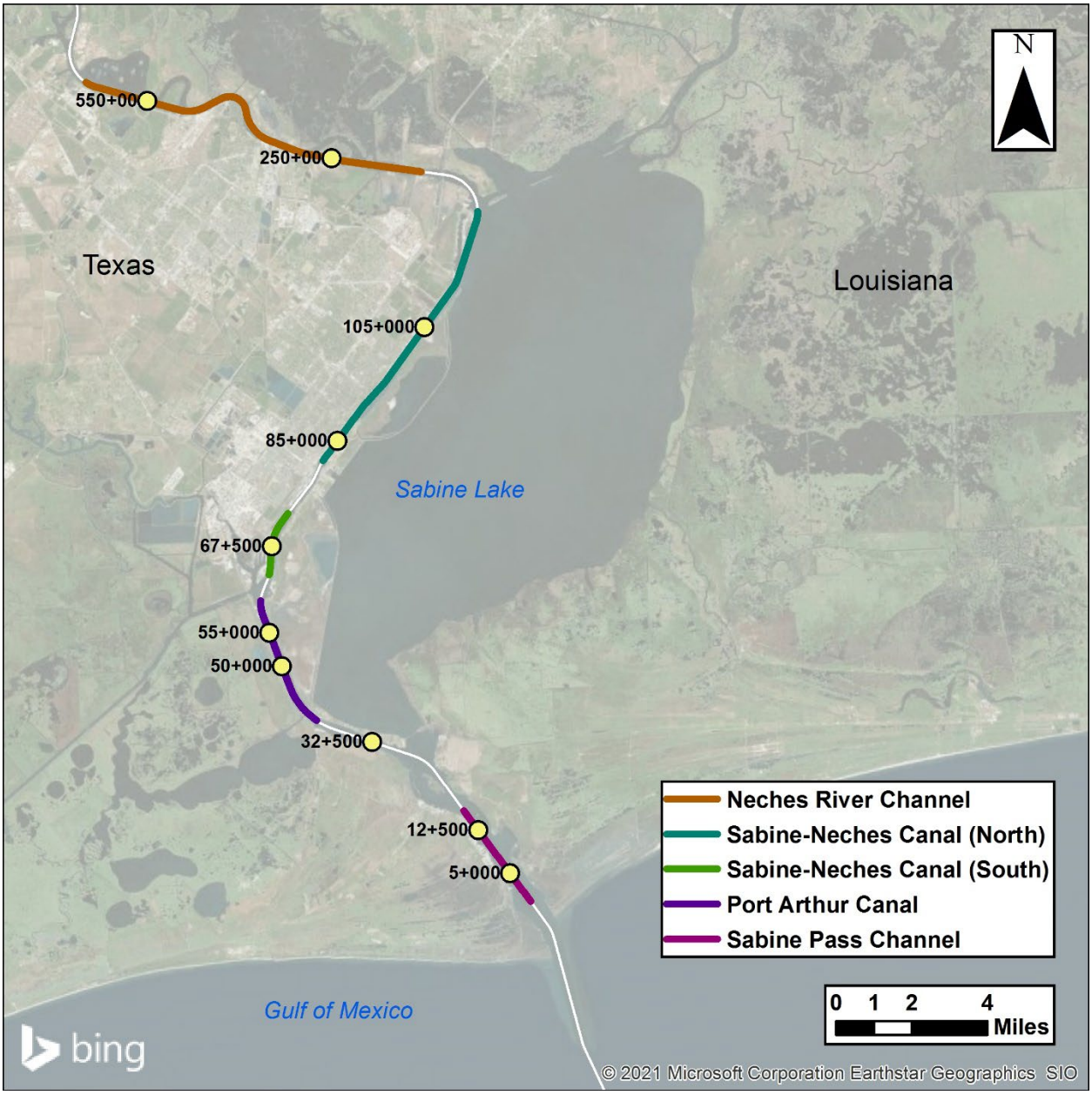

Figure 6-1
Model Save Point Locations Along SNWW Channel Centerline

Note: The color coding does not capture the full extent of each reach; rather, it refers to the name of the reach where each of the widening areas are considered.

Plots in Figure 6-2 and Figure 6-3 show the hydrodynamic response of water level and velocity at the model save point location for each of the three scenarios described in Section 4.5. The time axis is plotted relative to model start time and is unchanged for all three scenarios since the location and speed (8 kts) of the boat forcing (pressure disturbance) is the same. For all results in this section, the data are extracted at the stated station location, but the exact extraction location is along the -3.5 m contour which may vary for the various channel configurations. This approach is applied because the hydrodynamics are directly related to depth and not evaluating results at the same depth could lead to misguided conclusions.

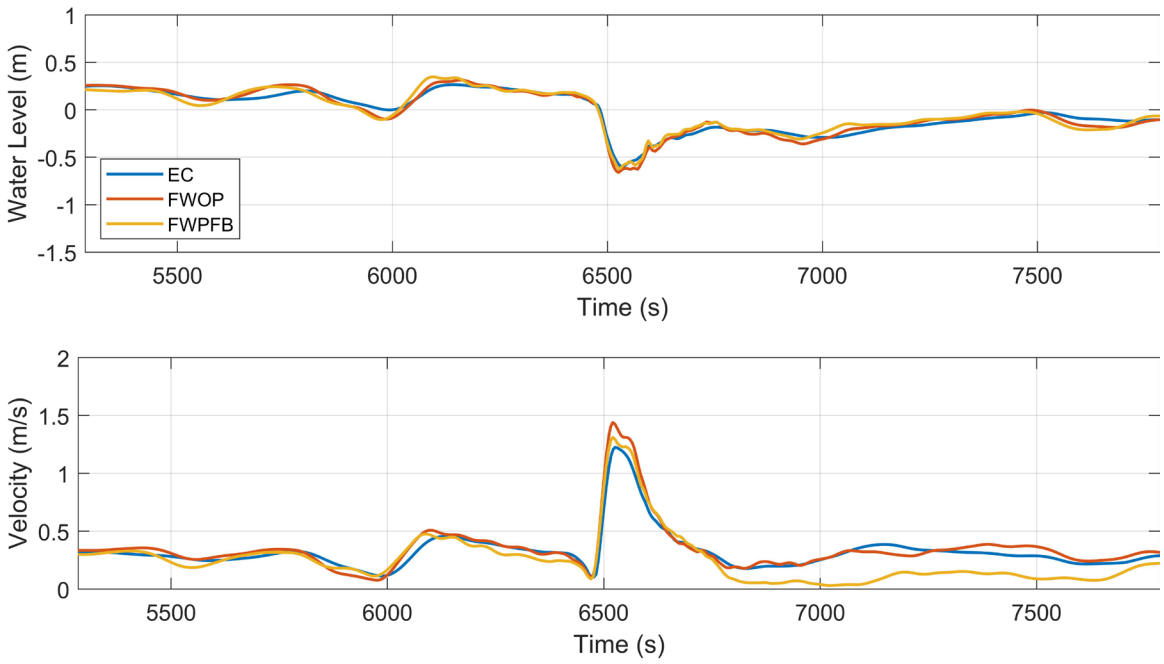

Figure 6-2
Time Series of Modeled Water Surface Elevation and Velocity from Save Point Located at Station 50+000 for EC, FWOP and FWPFB

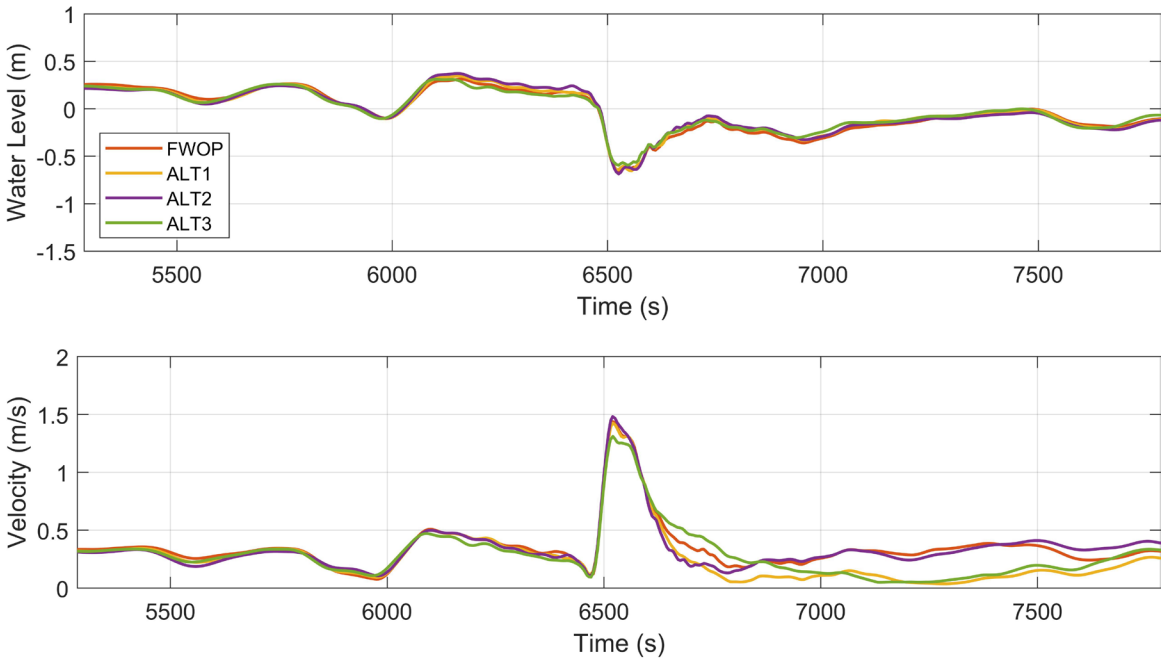

Figure 6-3
Time Series of Modeled Water Surface Elevation and Velocity from Save Point Located at Station 50+000 for FWOP, ALT1, ALT2, and ALT3.

Figure 6-2 shows the time series extracted at station 50+000. The shape of the time series for water level shows the bow wake preceding a drawdown as was seen in the calibration runs and field measurements. The velocity plot shows a small peak in velocity aligning with the bow wake, followed by a drop in the velocity associated with the current switching directions, and then the main peak of the velocity corresponding to the timing of the drawdown. Following the peak velocity, the velocity returns to a lower value but continues to rise and fall. This fluctuation is associated with the model returning to equilibrium in this area after the transiting vessel event and this part of the time series after the main drawdown was not used in this analysis. In general, the model results match the expected theoretical response and the measurements of the primary wave hydrodynamics (drawdown and return currents) that are generated by passing vessels in the SNWW with the exception of the surge which is evaluated in Section 6.5.

Comparing the individual runs in Figure 6-2 shows small differences. Looking specifically at the drawdown, all runs are very close showing a drop to -0.6 m. Model results are tabulated later in this section for closer review, but from the figure the difference in drawdown between the EC, FWOP, and FWPFB appears to be less than 0.1 m. The velocity comparisons also show minimal difference with the peak velocity highest for the FWOP condition, followed by the FWPFB, and finally the EC having the lowest peak velocity.

Figure 6-3 shows a similar result as Figure 6-2 with FWOP and all three alternatives having nearly the same drawdown. For the velocity comparisons FWOP, ALT1, and ALT2 have nearly identical peak velocities where ALT3 is lower by approximately 0.2 m/s. Note from Table 3-1 that ALT1 and ALT2 do not have any proposed changes at Station 50+000 and therefore the lack of differences in the model results compared to FWOP is expected. Time series for water level and velocity at Station 85+000 are shown in Figure 6-4 and Figure 6-5.

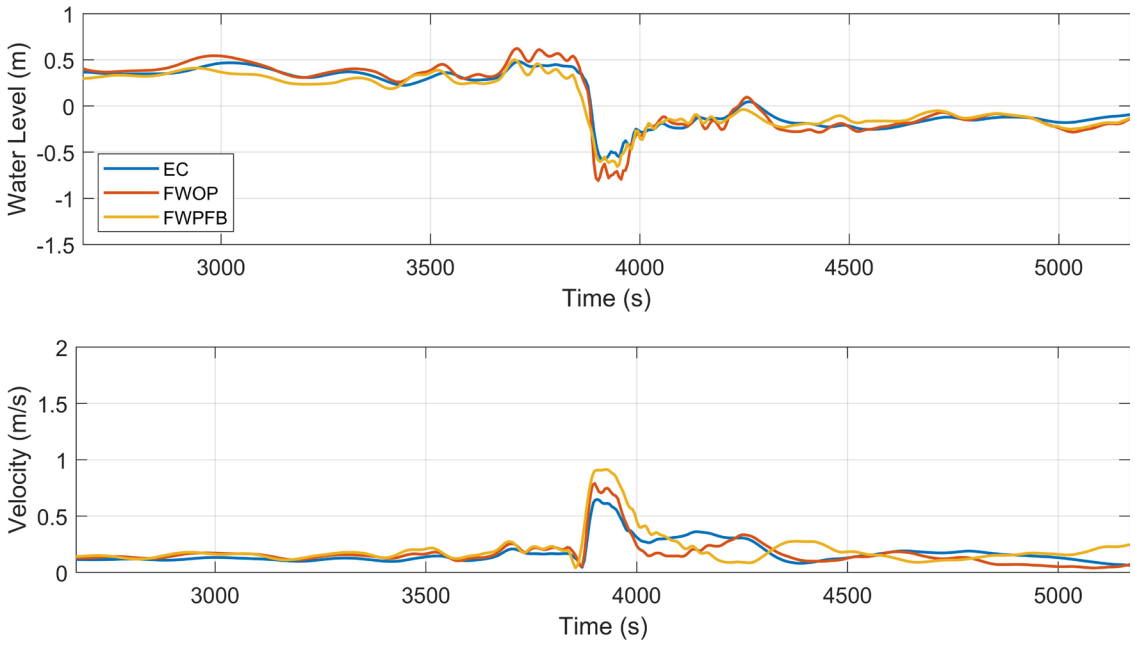

Figure 6-4
Time Series of Modeled Water Surface Elevation and Velocity from Save Point Located at Station 85+000 for EC, FWOP and FWPFB

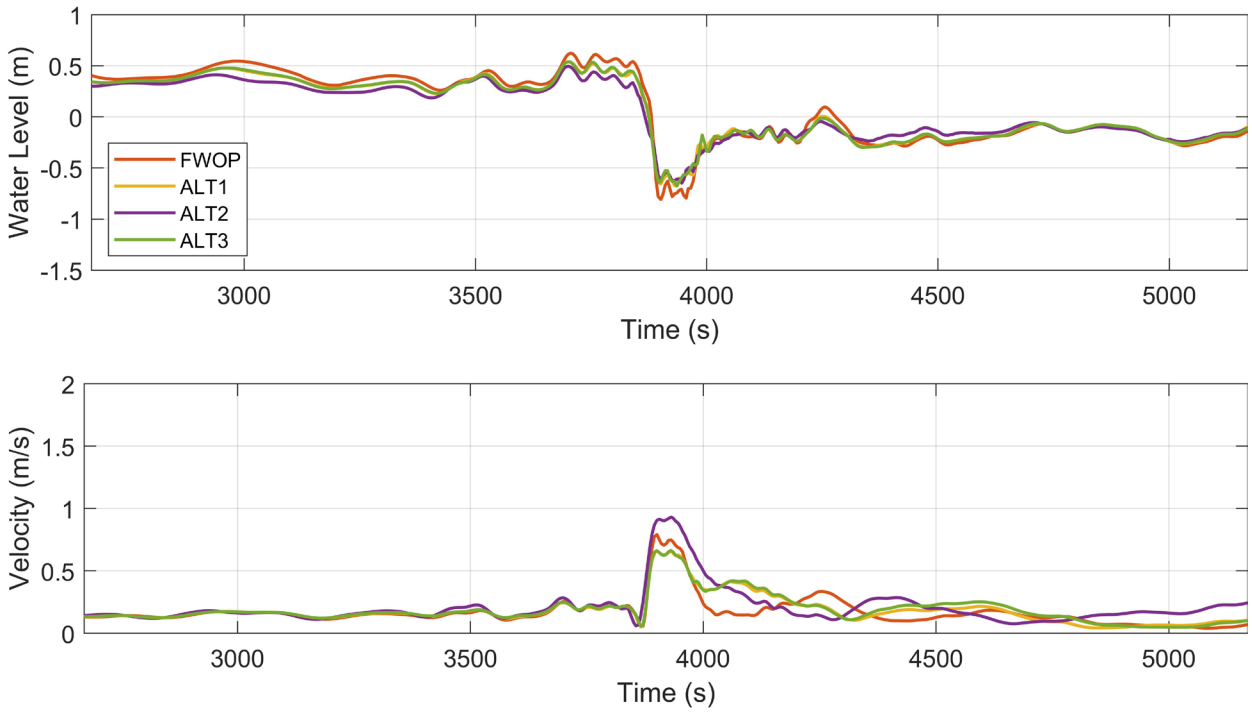

Figure 6-5
Time Series of Modeled Water Surface Elevation and Velocity from Save Point Located at Station 85+000 for FWOP, ALT1, ALT2, and ALT3

Comparison of the different model scenarios at Station 85+000 shows more variability in the drawdown and return currents than at Station 50+000. For example, at Station 85+000 shown in both Figure 6-4 and Figure 6-5, FWOP has the largest drawdown over the EC and any of the proposed widening alternatives. However, the relationship switches in the velocity plot with the FWPFB condition having a peak velocity of approximately 0.8 m/s while the FWOP peaks at approximately 0.7 m/s. In Figure 6-5 ALT2 has a peak velocity of approximately 0.9 m/s, same as FWPFB. This result is expected as the FWPFB and ALT2 have the same width at Station 85+000 while ALT1 and ALT3 are 100 ft narrower. Vessel hydrodynamics are expected to decrease with the wider channel width, so this result is abnormal. After further evaluation of the model results, the extraction point at Station 85+000 for ALT2 and FWPFB was pushed closer to the edge of the waterway as the location was specific to the -3.5 m contour. This adjustment in location put the extraction point in more focused return current against the channel bank which is expected to be the reason for the increased return current in the wider channels. Additional channel locations are investigated in Table 6-1 through Table 6-4.

Comparison of the EC run to the FWOP showed small increases in drawdown and peak velocity in both Figure 6-2 and Figure 6-4. It is important to consider that the vessel draft is varied between the two conditions because of the channel deepening. Therefore, the comparison is not direct, but still provides insight in potential changes in vessel hydrodynamics between the EC and FWOP channel configurations. The results from this analysis show a moderate increase in drawdown and return current for the FWOP channel, but because the FWOP channel is deeper, the model applied a deeper draft vessel while holding the velocity constant between the two conditions. Maynord

(2003) found similar results of an increase in return current between existing and proposed, but the modeled comparisons used a constant vessel draft and increased the vessel velocity in the proposed channel. The changes associated with deepening the channel are captured in the SNWW CIP (USACE 2011) and therefore are already considered in the ongoing design and construction.

The time series at the 10 save points all showed similar trends as those presented in Figure 6-2 and Figure 6-4, but further discussion regarding the comparisons of the different runs is provided next in the context of the tabulated quantified results of drawdown and return current values. These extrema of the drawdown and return current timeseries are presented in Table 6-1 and Comparison B is used to describe comparisons between FWOP and each of the FWP scenarios, i.e., FWPFB (Comparison "B") and ALT1, ALT2, and ALT3 (Comparisons "B1 to B3").

Table 6-3, respectively, and the comparisons A and B described in Section 4.5 presented as the difference between extrema (drawdown or return current) are shown in Table 6-2 and Table 6-4. At the bottom of each table, mean values are given to indicate general trends for comparisons. Recall the modeled vessel speed was 8 kts for all conditions and the draft increased from 36 ft for EC to 44 ft for all other conditions.

Table 6-1
Modeled Drawdown Calculated from Save Point Location Time Series

Reach	Station	Drawdown (m)					
		Existing (36 ft)	FWOP (44 ft)	FWPFB (44 ft)	ALT1 (44 ft)	ALT2 (44 ft)	ALT3 (44 ft)
Sabine Pass Channel	5+000	0.3	0.4	0.4	0.4	0.4	0.4
	12+500	0.2	0.2	0.2	0.2	0.2	0.2
Port Arthur Canal	32+500	0.5	0.5	0.6	0.5	0.6	0.5
	50+000	0.6	0.7	0.6	0.7	0.7	0.6
	55+000	0.5	0.6	0.6	0.6	0.7	0.6
Sabine-Neches Canal	67+500	0.6	0.7	0.6	0.6	0.6	0.6
	85+000	0.6	0.8	0.7	0.7	0.6	0.7
	105+000	0.9	1.2	0.5	0.8	0.5	0.7
Neches River Channel	250+00	0.4	0.6	0.7	0.6	0.7	0.6
	550+00	0.7	0.9	0.7	0.8	0.7	0.9
Mean:		0.5	0.7	0.6	0.6	0.6	0.6

* Note: Variances smaller than the Mean Absolute Model Error of 0.15 m are not precise (calculated in Section 5.4).

Table 6-2
Differences in Modeled Drawdown Calculated from Save Point Location Time Series

Reach	Station	Drawdown Comparisons (m)				
		A	B	B1	B2	B3
Sabine Pass Channel	5+000	0.1	0.0	0.0	0.0	0.0
	12+500	0.0	0.0	0.0	0.0	0.0
Port Arthur Canal	32+500	0.0	0.0	0.0	0.1	0.0
	50+000	0.1	0.0	0.0	0.0	-0.1
	55+000	0.2	-0.1	0.0	0.0	-0.1
Sabine-Neches Canal	67+500	0.2	-0.1	-0.1	-0.1	-0.1
	85+000	0.2	-0.2	-0.1	-0.2	-0.1
	105+000	0.3	-0.7	-0.4	-0.7	-0.4
Neches River Channel	250+00	0.1	0.1	0.0	0.1	0.0
	550+00	0.3	-0.2	-0.1	-0.2	0.0
Mean:		0.1	-0.1	0.0	0.0	0.0

* Note: Variances smaller than the Mean Absolute Model Error of 0.15 m are not precise (calculated in Section 5.4).

As described earlier, the analysis of the model scenarios is broken down into paired comparisons summarized as follows:

- Comparison A: Increasing the depth of the channel and the draft of the vessel (EC to FWOP) with the same 8 kts vessel speed. This vessel speed is approximately 90 percent of the limit speed for EC and FWOP.
- Comparison B: Increasing the width of the channel (FWOP to FWP) using the same vessel speed and draft. The wider channel increases the limit speed such that 8 kts is 74 percent. Comparison B is used to describe comparisons between FWOP and each of the FWP scenarios, i.e., FWPFB (Comparison "B") and ALT1, ALT2, and ALT3 (Comparisons "B1 to B3").

Table 6-3
Modeled Return Current Calculated from Save Point Location Time Series

Reach	Station	Return Current (m/s)					
		Existing (36 ft)	FWOP (44 ft)	FWPFB (44 ft)	ALT1 (44 ft)	ALT2 (44 ft)	ALT3 (44 ft)
Sabine Pass Channel	5+000	0.6	0.8	0.7	0.8	0.8	0.8
	12+500	0.4	0.5	0.4	0.5	0.5	0.4
Port Arthur Canal	32+500	1.1	1.2	1.2	1.2	1.2	1.2
	50+000	1.2	1.4	1.3	1.4	1.5	1.3
	55+000	1.3	1.3	1.2	1.3	1.3	1.2
Sabine-Neches Canal	67+500	1.4	1.8	1.4	1.6	1.4	1.6
	85+000	0.6	0.8	0.9	0.7	0.9	0.7
	105+000	1.0	1.2	0.9	1.4	0.9	1.4
Neches River Channel	250+00	0.9	0.9	1.0	0.9	1.0	1.0
	550+00	1.8	2.2	2.0	2.1	2.0	2.1
Mean:		1.0	1.2	1.1	1.2	1.2	1.2

* Note: Variances smaller than the Mean Absolute Model Error of 0.10 m/s are not precise (calculated in Section 5.4).

Table 6-4
Differences in Modeled Return Current Calculated from Save Point Location Time Series

Reach	Station	Return Current Comparisons (m/s)				
		A	B	B1	B2	B3
Sabine Pass Channel	5+000	0.2	0.0	0.0	0.0	0.0
	12+500	0.1	0.0	0.0	0.0	0.0
Port Arthur Canal	32+500	0.1	0.0	0.0	0.0	0.0
	50+000	0.2	-0.1	0.0	0.0	-0.1
	55+000	0.0	0.0	0.1	0.1	-0.1
Sabine-Neches Canal	67+500	0.4	-0.3	-0.2	-0.3	-0.2
	85+000	0.1	0.1	-0.1	0.1	-0.1
	105+000	0.2	-0.3	0.2	-0.3	0.1
Neches River Channel	250+00	0.0	0.1	0.0	0.1	0.1
	550+00	0.4	-0.2	0.0	-0.2	0.0
Mean:		0.2	-0.1	0.1	0.0	0.0

* Note: Variance smaller than the Mean Absolute Model Error of 0.10 m/s are not precise (calculated in Section 5.4).

The drawdown and return currents in Table 6-1 and Comparison B is used to describe comparisons between FWOP and each of the FWP scenarios, i.e., FWPFB (Comparison "B") and ALT1, ALT2, and ALT3 (Comparisons "B1 to B3").

Table 6-3 indicate a modest increase in vessel effects between EC and FWOP (comparison A). The mean drawdown increases 0.14 m (0.51 m to 0.66 m) and the return current increases 0.17 m/s (approximately 1.1 m/s to 1.2 m/s). Although the ship speed is the same and is near 90 percent of the limiting speed for the narrow reaches of the channel, the blockage ratio is higher for the FWOP scenarios because the vessel is drafting deeper within the deeper channel. The effect of this condition is especially noticed in the narrower reaches of the channel, and therefore an increase in the hydraulic parameters is expected. This result should not be confused with a comparison of a 36 ft draft vessel in both the EC and FWOP channel conditions, for which reduced effects in the FWOP channel are expected. This scenario was not modeled, but the reduction of drawdown and return current from decreasing the blockage ratio (same vessel cross-section and a larger channel cross-section) is well established and supported by the Schijf equations.

Comparison B (FWOP and FWP, both conditions at 8 kts) demonstrates a reduction of vessel effects for a widening the channel when the same vessel, draft depth, and speed is modeled. The vessel effects from FWOP to FWPFB are reduced by 0.11 m for drawdown and 0.07 m/s for return currents. The reductions are less for the three alternatives. Modeled vessel draft has the greatest influence on the drawdown and return current based on these results. This conclusion is also supported by Maynord (2003), along with a strong dependency on vessel speed. Although even faster speeds do occur, such as the lightly loaded (8.1 m draft) Star Luster calibration vessel observed traveling near 10.5 kts, the heavily loaded Suezmax vessels will not travel as fast but theoretically can produce the largest hydrodynamic effects.

Note the Mean Absolute Model Error was calculated to be 0.15 m and 0.10 m/s for the peak drawdown and max return current, respectively. While the mean differences between the channel configurations fall below the Mean Absolute Error, the potential limitation of the Mean Absolute Error calculation are discussed in Section 5.4. The results discussed in this report are expected to qualitatively represent the differences between the vessel hydrodynamics for the channel configurations modeled and align with theory. Although, the model results do support these changes will be small and will have limited to no impact on the bank erosion (see Section 6.6).

An additional analysis of Comparison B was made for the area surrounding save point 85+000 in Sabine-Neches Canal North to show the spatial differences in the models and present further understanding of the reason for the increased peak return current in the widened channel. Plan view graphics of the model results for the modeled bathymetry elevations, velocities, and water levels near the time of the most intense conditions are presented in Figure 6-6, Figure 6-7, and Figure 6-8.

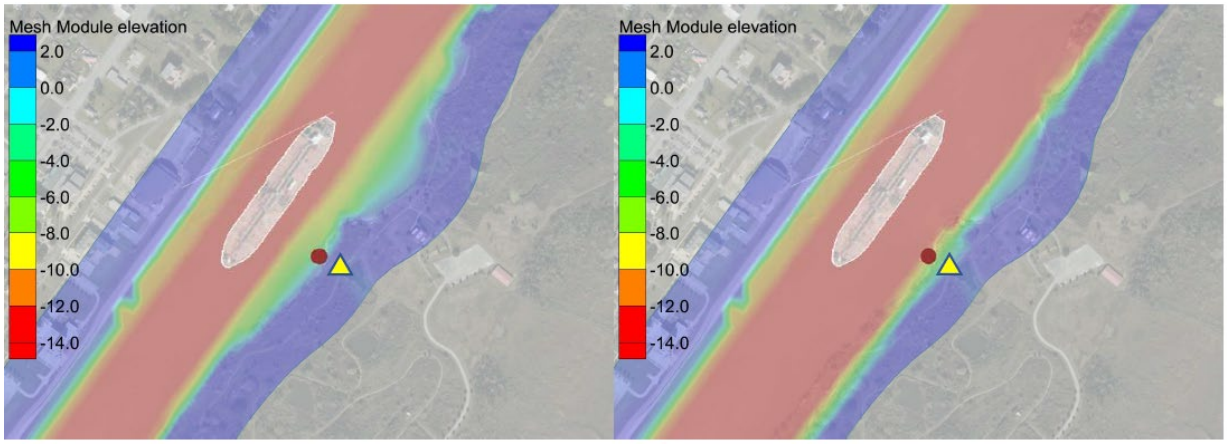

Figure 6-6: Model Bathymetry Elevation Near Station 85+000 Extraction Point Sabine-Neches Canal North for FWOP Left and FWPFB Right

(The Save Point Location at the 3 m Depth Contour is Given by a Circle for the FWOP and a Triangle for FWPFB)

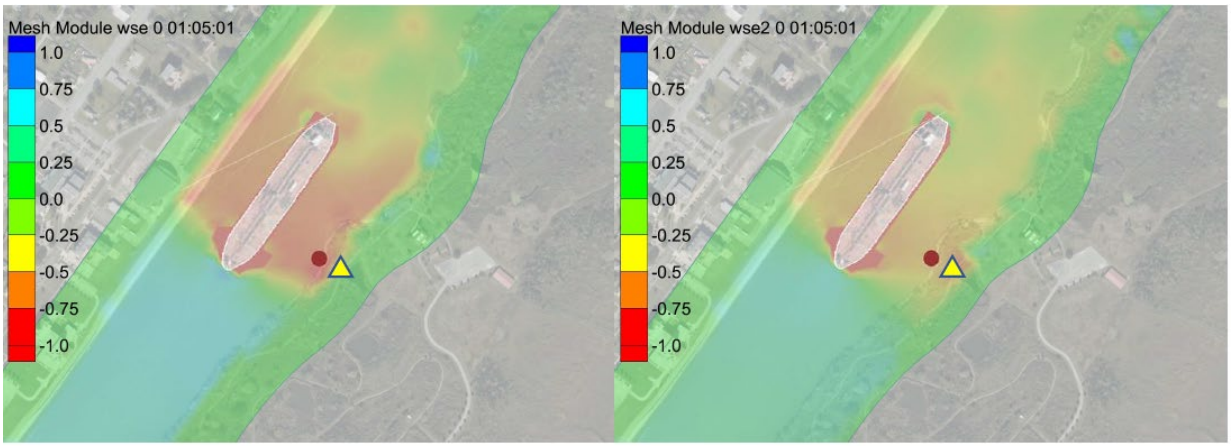

Figure 6-7: Modeled Water Level Near 85+000 Extraction Point Sabine-Neches Canal North for FWOP Left and FWPFB Right

(The Save Point Location at the 3 m Depth Contour is Given by a Circle for the FWOP and a Triangle for FWPFB)

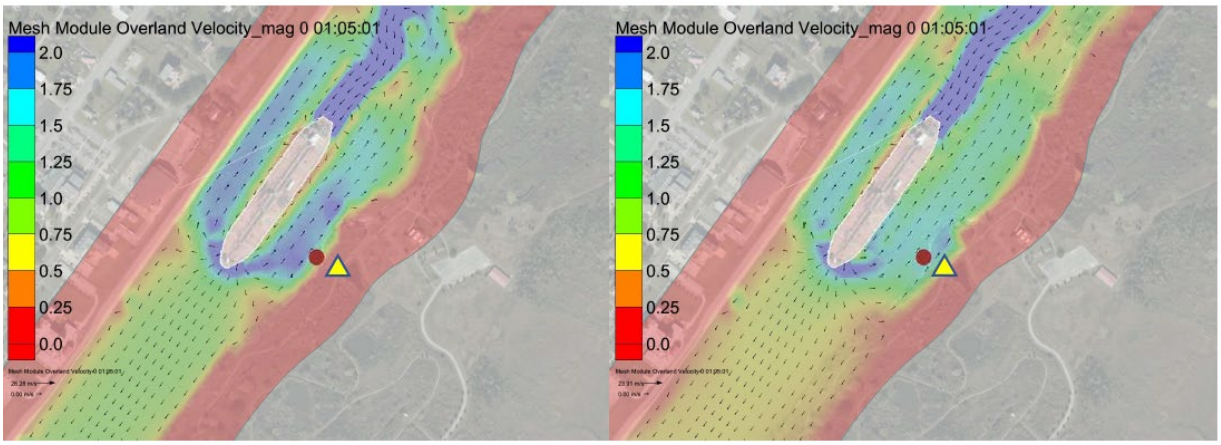

Figure 6-8: Modeled Velocity Near 85+000 Extraction Point Sabine-Neches Canal North for FWOP Left and FWPFB Right

(The Save Point Location at the 3 m Depth Contour is Given by a Circle for the FWOP and a Triangle for FWPFB)

The left-hand side of these figures presents the FWOP condition and the right-hand side the FWPFB condition. The reduction of drawdown and return current due to the widening is evident when looking at the average values across the channel. For example, Figure 6-6 shows the widened channel on the right as shown by the red contour. The effects of the widened channel are seen for the same modeled vessel draft and speed in Figure 6-7 and Figure 6-8 and a reduction in the drawdown (red) and return current (blue) areas respectively.

These figures also highlight the need to use a point at a consistent water depth when making comparisons between the models. For example, the widened channel shifts the location of the 3 m contour (where the timeseries is analyzed) away from the channel. The 3.5 m depth contour is located at the red circle for the FWOP condition and the yellow triangle for the FWPFB condition.

6.2 Analysis 2: Channel Averaged Peak Velocity and Drawdown

This analysis compares the model results within the channel along the entire waterway. The processing method includes the following steps.

1. Calculate the maximum velocity and the minimum water level at each model node which are taken to be the peak drawdown and the peak return current. Note the max water level, or transverse stern wave, is discussed in Section 6.5.
2. Construct perpendicular cross-sections along the channel centerline at 100 ft intervals.
3. Interpolate the peak drawdown onto the cross-section lines.
4. Mask data along each cross-section that lies within half a beam width of the vessel and outside of the FWOP channel toe.
5. Average the drawdown and return current along each cross-section and plot versus channel stationing.

This approach is consistent with the Schijf equation formulation, where the hydrodynamic vessel effects are given as the average water level and velocity within the channel. The benefit of this analysis is the relative changes are shown along the full length of channel, not just at particular locations as was done in previous feasibility studies (USACE, 2008) and Section 6.1 of this report. The full results after step 5 are presented in Figure 6-9 through Figure 6-10 showing drawdown and return current along the entire SNWW for all four modeled scenarios.

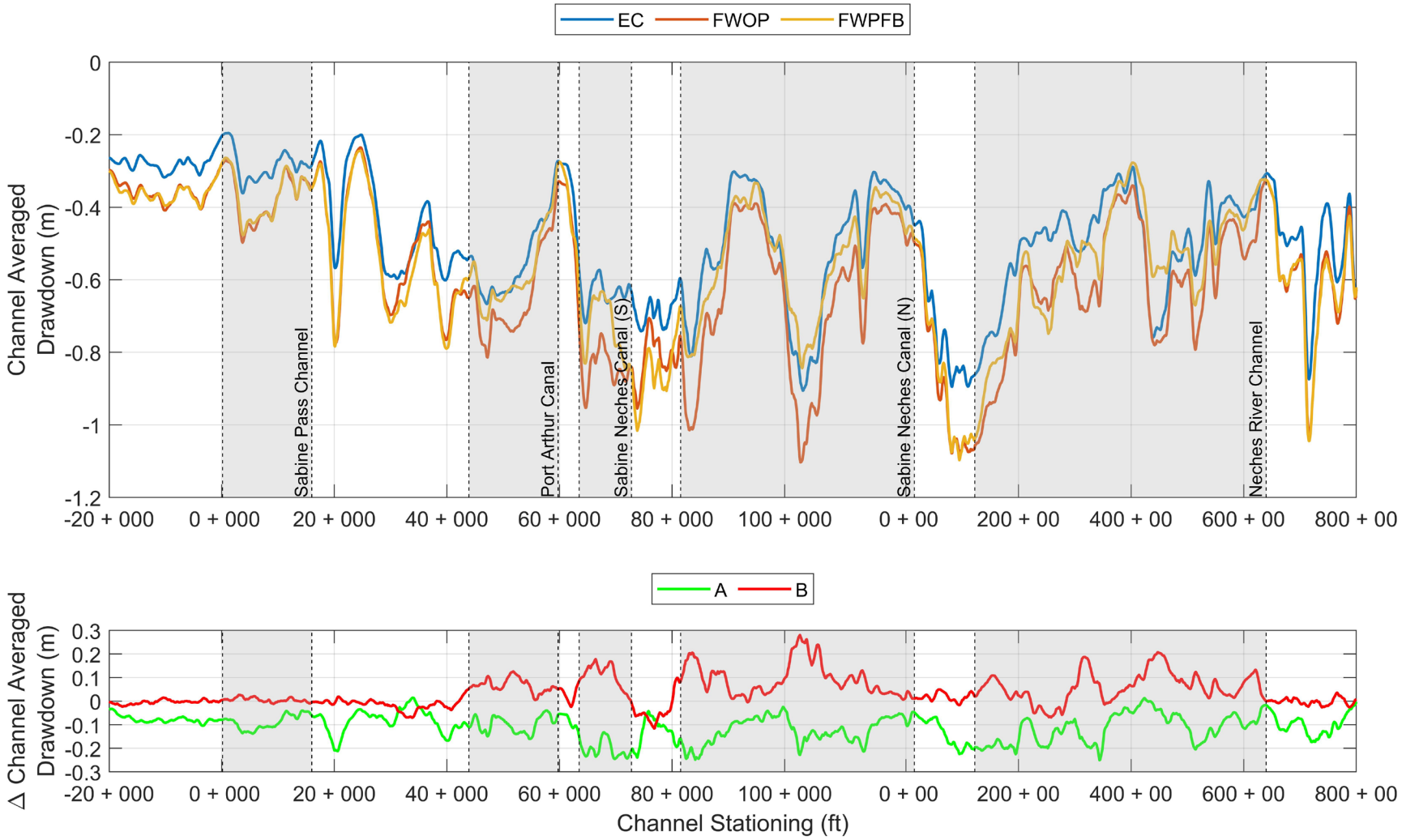

Figure 6-9: Channel Averaged Drawdown Versus Stationing from AdH Model for EC, FWOP, and FWPFB. Gray Areas of Plot Indicate Locations of Proposed Widening

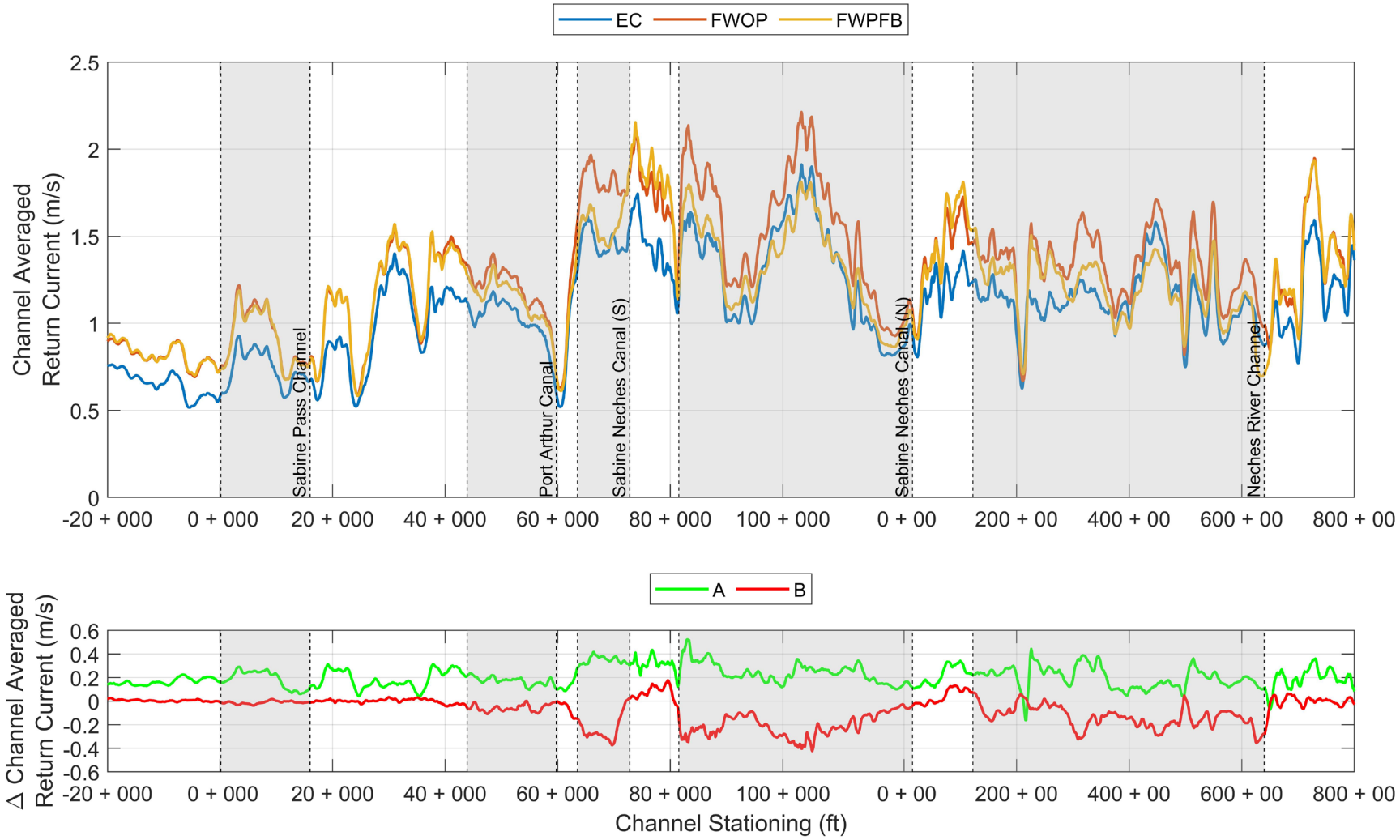

Figure 6-10: Channel Averaged Return Current Versus from AdH Model for EC, FWOP, and FWPFB. Gray Areas of Plot Indicate Locations of Proposed Widening

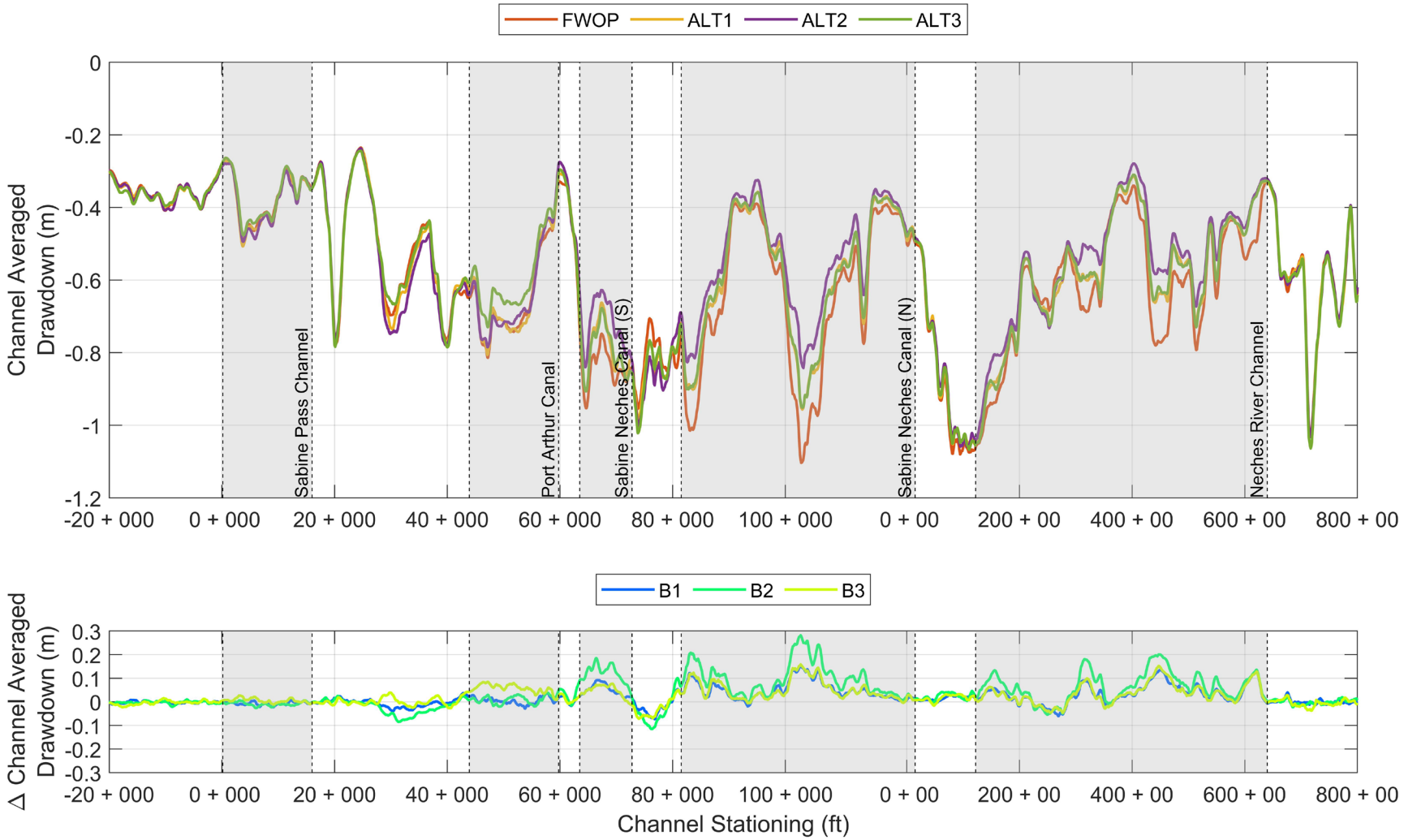

Figure 6-11: Channel Averaged Drawdown Versus Stationing from AdH Model for FWOP, ALT1, ALT2 and ALT3. Gray Areas of Plot Indicate Locations of Proposed Widening.

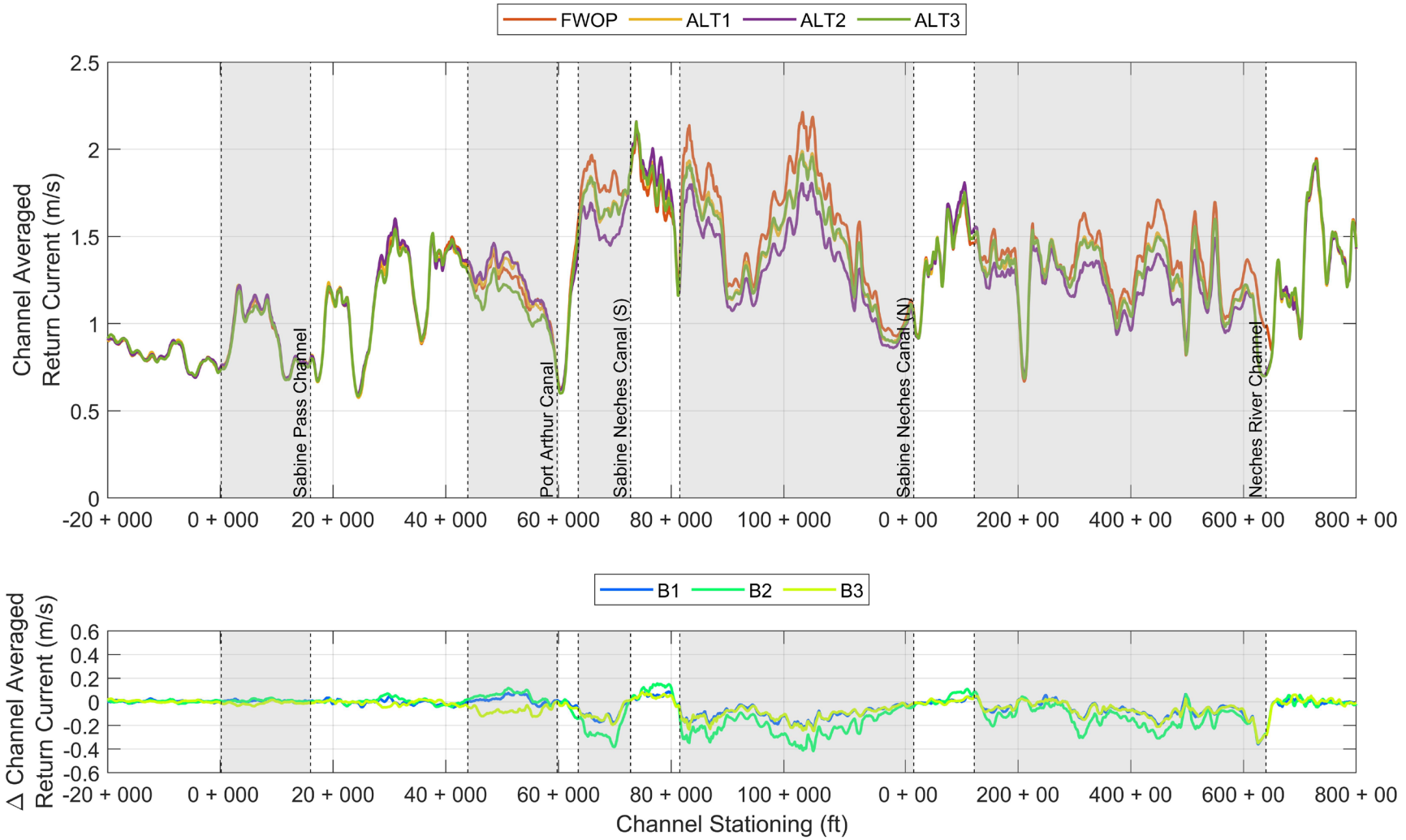

Figure 6-12: Channel Averaged Return Current Versus Stationing from AdH Model for FWOP, ALT1, ALT2 and ALT3. Gray Areas of Plot Indicate Locations of Proposed Widening.

The general trends observed from analysis 2 are consistent with results found from analysis 1 (Section 6.1) with an average increase in predicted changes to drawdown and return currents from EC to FWOP, and a decrease in predicted changes to drawdown and return currents from FWOP to FWP 8 kts. Overall trends are investigated by averaging the channel averaged drawdown and return current over the full SNWW from Sabine Pass to Beaumont. These averages for analysis 2 are obtained as the mean of Figure 6-9 and Figure 6-10 along the entire channel and are given in Table 6-5 and Table 6-6. The comparisons are repeated as described in Section 4.5 and detailed in Figure 4-5. Comparison A again shows a modest increase in vessel effects from EC to FWOP. Here the deeper vessel draft overcompensates for the decrease in predicted changes to drawdown and return currents caused by the channel deepening. In Comparison B, results show a slight reduction or no change in vessel effects from channel widening when the vessel parameter remain constant. Comparison B is the most relevant for assessing changes resulting from the FWP because the effects of widening the channel are isolated and demonstrate a reduction in vessel effects.

Table 6-5
Modeled Channel Averaged Drawdown and Return Currents Averaged Along Entire SNWW Reach

	EC	FWOP	FWPFB	ALT1	ALT2	ALT3
Drawdown (m)	0.5	0.6	0.6	0.6	0.6	0.6
Return Current (m/s)	1.2	1.4	1.3	1.3	1.3	1.3

* Note: Variances smaller than the Mean Absolute Model Error of 0.15 m are not precise (calculated in Section 5.4).

Table 6-6
Modeled Channel Averaged Drawdown and Return Currents Averaged Along Entire SNWW Reach

	A	B	B1	B2	B3
Drawdown (m)	0.1	0.0	0.0	0.0	0.0
Return Current (m/s)	0.2	-0.1	0.0	-0.1	-0.1

* Note: Variances smaller than the Mean Absolute Model Error of 0.15 m are not precise (calculated in Section 5.4).

6.3 Repeat Analysis 1 for Sea Level Change Scenarios: FWOP and FWP

The same approach described in Sections 6.1 and 6.2 was repeated for the future relative sea level change (RSLC) scenarios described in Section 4.5. Corresponding to the "high" 50-yr scenario described in Table 4-2 and Figure 4-7, 1.43 m of water level was added when initializing the model, i.e., the water level was set at +0.43 m NAVD88 corresponding to the approximate 2020 mean sea level and an additional 1.0 m was added for RSLC. The time series of near bank water level and velocity are again presented for 50+000 located in the Port Arthur Canal (Figure 6-13) and 85+000 located in the Sabine-Neches Canal North (Figure 6-15). The still water level for these scenarios is 1.43 m NAVD88 to represent RSLC. Also, the same save point locations used as previously were translated towards the bank, such that these time-series remain at the 3.5 m depth contour (relative to the initial still water level). As seen previously for the FWOP and FWOPFB cases, the time series show similar vessel effects. Note, because the RSLC analysis was only performed on the central mesh, not all the comparisons shown in Section 6.1 are presented in this section.

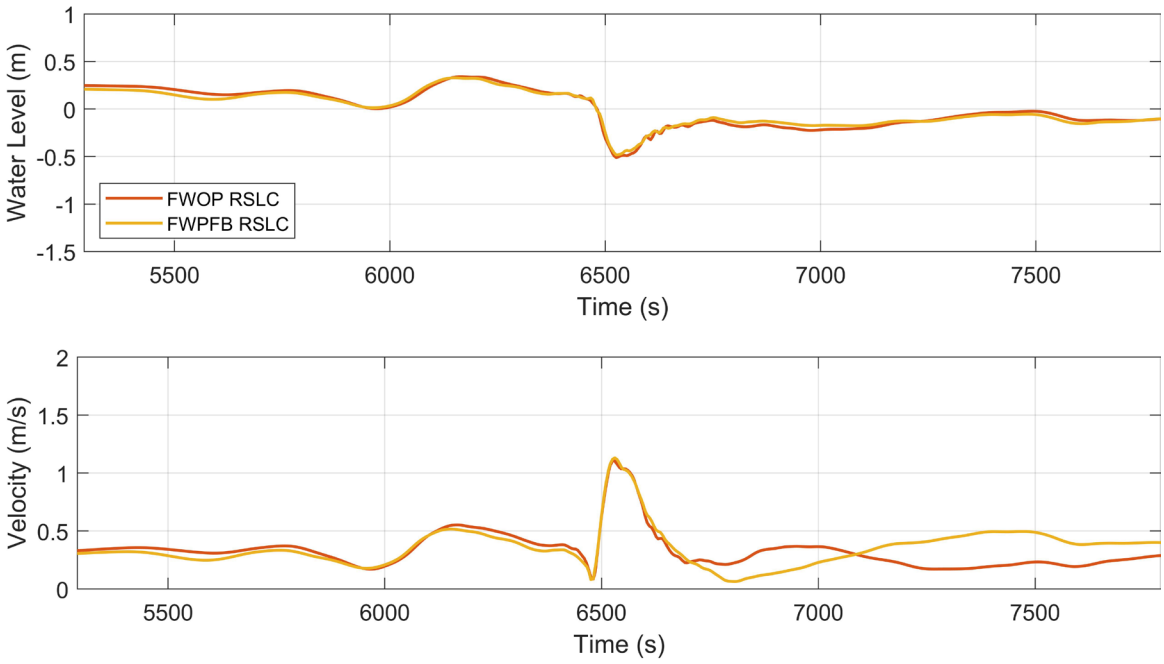

Figure 6-13
Time Series of Modeled Water Surface Elevation and Velocity from Save Point Located at Station 50+000 for FWOP and FWPFB Including RSLC

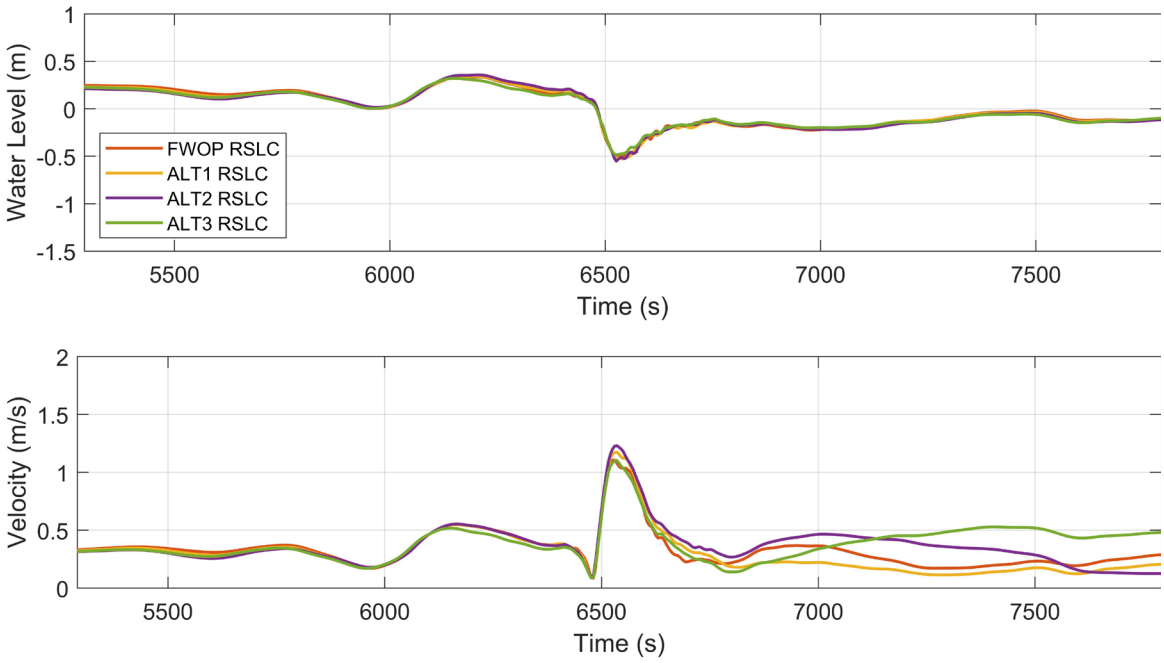

Figure 6-14
Time Series of Modeled Water Surface Elevation and Velocity from Save Point Located at Station 50+000 for FWOP, ALT1, ALT2, and ALT3 Including RSLC

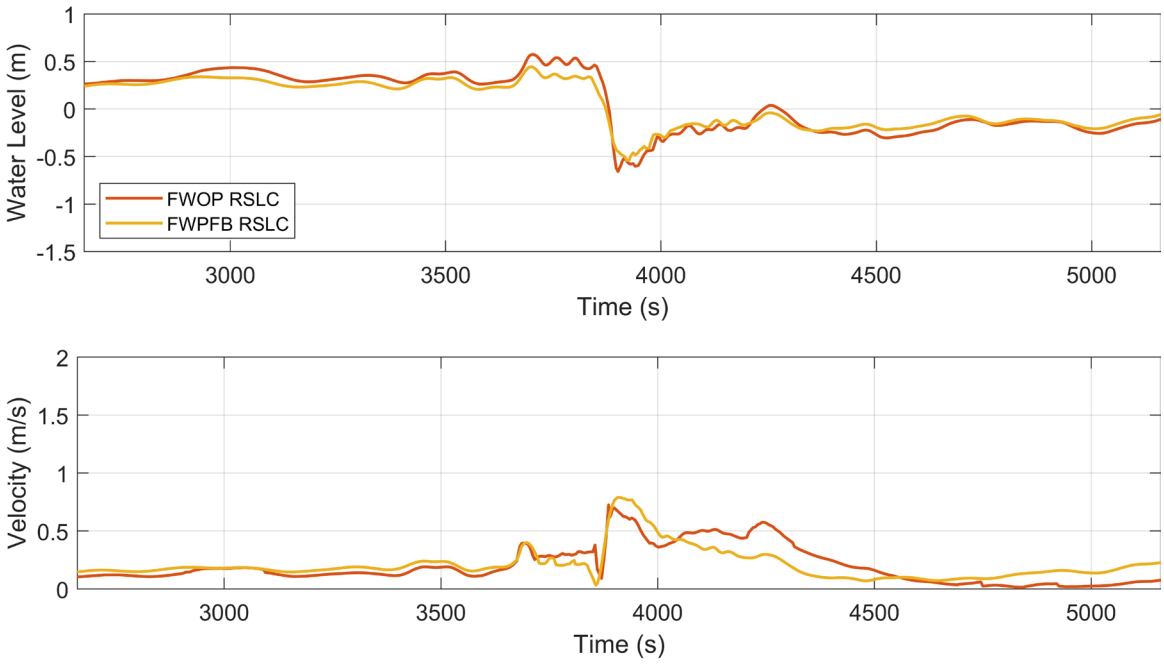

Figure 6-15
Time Series of Modeled Water Surface Elevation and Velocity at Save Point Located at Station 85+000 for FWOP and FWPFB Including RSLC

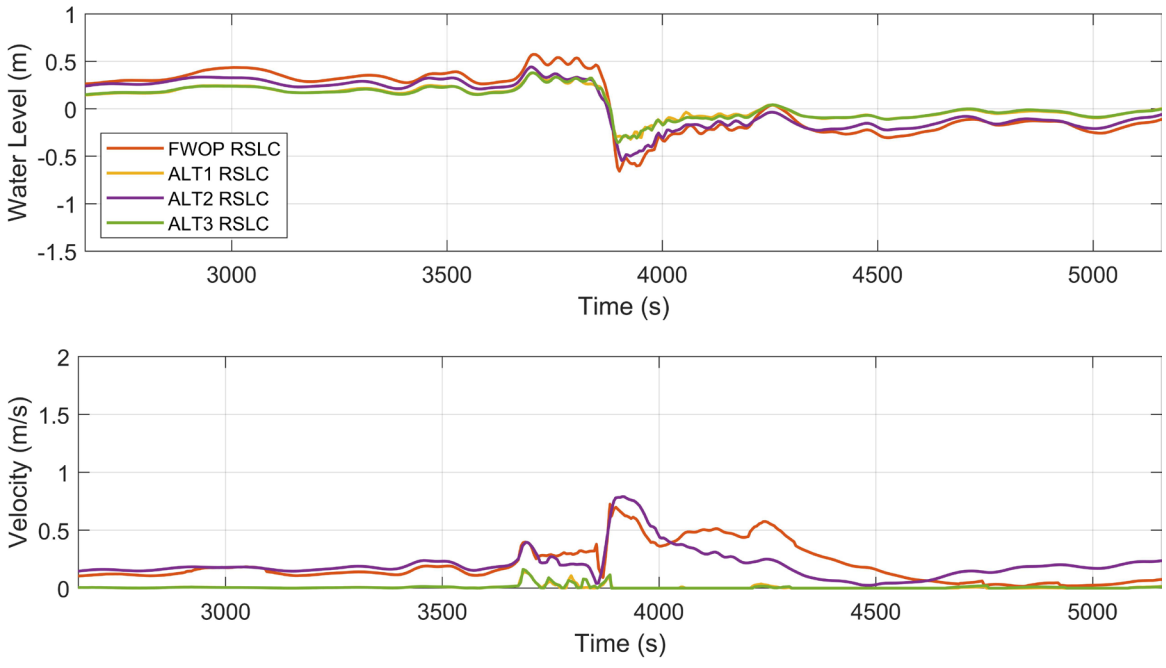

Figure 6-16
Time Series of Modeled Water Surface Elevation and Velocity from Save Point Located at Station 85+000 for FWOP, ALT1, ALT2, and ALT3 Including RSLC

Peak results for drawdown and return current are tabulated and presented in Table 6-1 and Table 6-2. The tabulated drawdowns are referenced to the 1.43 m initial still water level. The RSLC does not qualitatively change the previous results where the FWP reduces the vessel effects when vessel speed does not change. The additional water level increases the channel area and is expected to reduce the magnitude of vessel effects, as seen before, and the variance between the channel configurations. Tabulated summaries of the model comparisons are provided in Table 6-7 through Table 6-10.

Table 6-7
Modeled Drawdown Calculated from Save Point Location Time Series for RSLC

Reach	Station	Drawdown (m)				
		FWOP	FWPFB	ALT1	ALT1	ALT1
		(44 ft)	(44 ft)	(44 ft)	(44 ft)	(44 ft)
Port Arthur Canal	32+500	0.6	0.6	0.6	0.6	0.6
	50+000	0.5	0.5	0.5	0.6	0.5
	55+000	0.5	0.4	0.5	0.5	0.5
Sabine-Neches Canal	67+500	0.5	0.4	0.5	0.4	0.5
	85+000	0.7	0.5	0.6	0.6	0.6
	105+000	0.8	0.4	0.8	0.4	0.8
Mean:		0.6	0.5	0.6	0.5	0.6

* Note: Variances smaller than the Mean Absolute Model Error of 0.15 m are not precise (calculated in Section 5.4).

Table 6-8
Difference in Modeled Drawdown Calculated from Save Point Location Time Series for RSLC

Reach	Station	Drawdown (m)			
		B	B1	B2	B3
Port Arthur Canal	32+500	0.0	0.0	0.0	0.0
	50+000	0.0	0.0	0.0	0.0
	55+000	-0.1	0.0	0.0	0.0
Sabine-Neches Canal	67+500	-0.1	0.0	0.0	0.0
	85+000	-0.1	-0.1	-0.1	0.0
	105+000	-0.4	0.0	-0.4	0.0
Mean:		-0.1	0.1	-0.1	0.1

* Note: Variances smaller than the Mean Absolute Model Error of 0.15 m are not precise (calculated in Section 5.4)..

Table 6-9
Modeled Return Current Calculated from Save Point Location Time Series

Reach	Station	Return Current (m/s)					
		Existing (36 ft)	FWOP (44 ft)	FWPFB (44 ft)	ALT1 (44 ft)	ALT2 (44 ft)	ALT3 (44 ft)
Sabine Pass Channel	5+000	0.6	0.8	0.7	0.8	0.8	0.7
	12+500	0.4	0.5	0.4	0.5	0.5	0.4
Port Arthur Canal	32+500	1.1	1.2	1.2	1.2	1.2	1.2
	50+000	1.2	1.4	1.3	1.4	1.5	1.3
	55+000	1.3	1.3	1.2	1.3	1.3	1.2
Sabine-Neches Canal	67+500	1.4	1.8	1.4	1.6	1.4	1.6
	85+000	0.6	0.8	0.9	0.8	1.5	0.8
	105+000	1.0	1.2	0.9	1.9	1.6	1.9
Neches River Channel	250+00	0.9	0.9	1.0	0.9	1.0	1.0
	550+00	1.8	2.2	2.0	2.1	2.0	2.1
Mean:		1.0	1.2	1.1	1.3	1.3	1.2

* Note: Variances smaller than the Mean Absolute Model Error of 0.10 m/s are not precise (calculated in Section 5.4).

Table 6-10
Differences in Modeled Return Current Calculated from Save Point Location Time Series

Reach	Station	Return Current Comparisons (m/s)			
		B	B1	B2	B3
Port Arthur Canal	32+500	0.0	0.0	0.0	0.0
	50+000	-0.1	0.0	0.0	-0.1
	55+000	0.0	0.1	0.1	-0.1
Sabine-Neches Canal	67+500	-0.3	-0.2	-0.3	-0.2
	85+000	0.1	0.0	0.7	0.0
	105+000	-0.2	0.8	0.5	0.7
Mean:		-0.1	0.1	0.0	0.0

* Note: Variances smaller than the Mean Absolute Model Error of 0.10 m/s are not precise (calculated in Section 5.4).

The results presented in Table 6-7 through Table 6-10Table 6-9 support the same conclusions seen in Section 6.1 with the widened channel generally resulting in small decreases to vessel hydrodynamics. Note in the comparison of ALT1 to ALT3 not all stations shown in the tables included widening which can skew the means presented in the table.

6.4 Repeat Analysis 2 for Sea Level Change Scenarios: FWOP and FWP

This analysis follows the same five processing steps described in Section 6.2, but repeated for the future RSLC scenarios describe in Section 4.5. This analysis compares the model results within the channel along reaches of the waterway contained in the central mesh. The RSLC scenario was run on the central mesh and with analysis extents between station 28+000 and 50+00 (from Sabine

Pass to approximately Rainbow Bridge). The results are presented in Figure 6-17 and Figure 6-18 showing drawdown and return current along reaches of the SNWW within the central mesh for the FWOP and FWPFB modeled future scenarios with RSLC. Results comparing drawdown and return current between FWOP and ALT1, ALT2, and ALT3 are presented in Figure 6-19 and Figure 6-20.

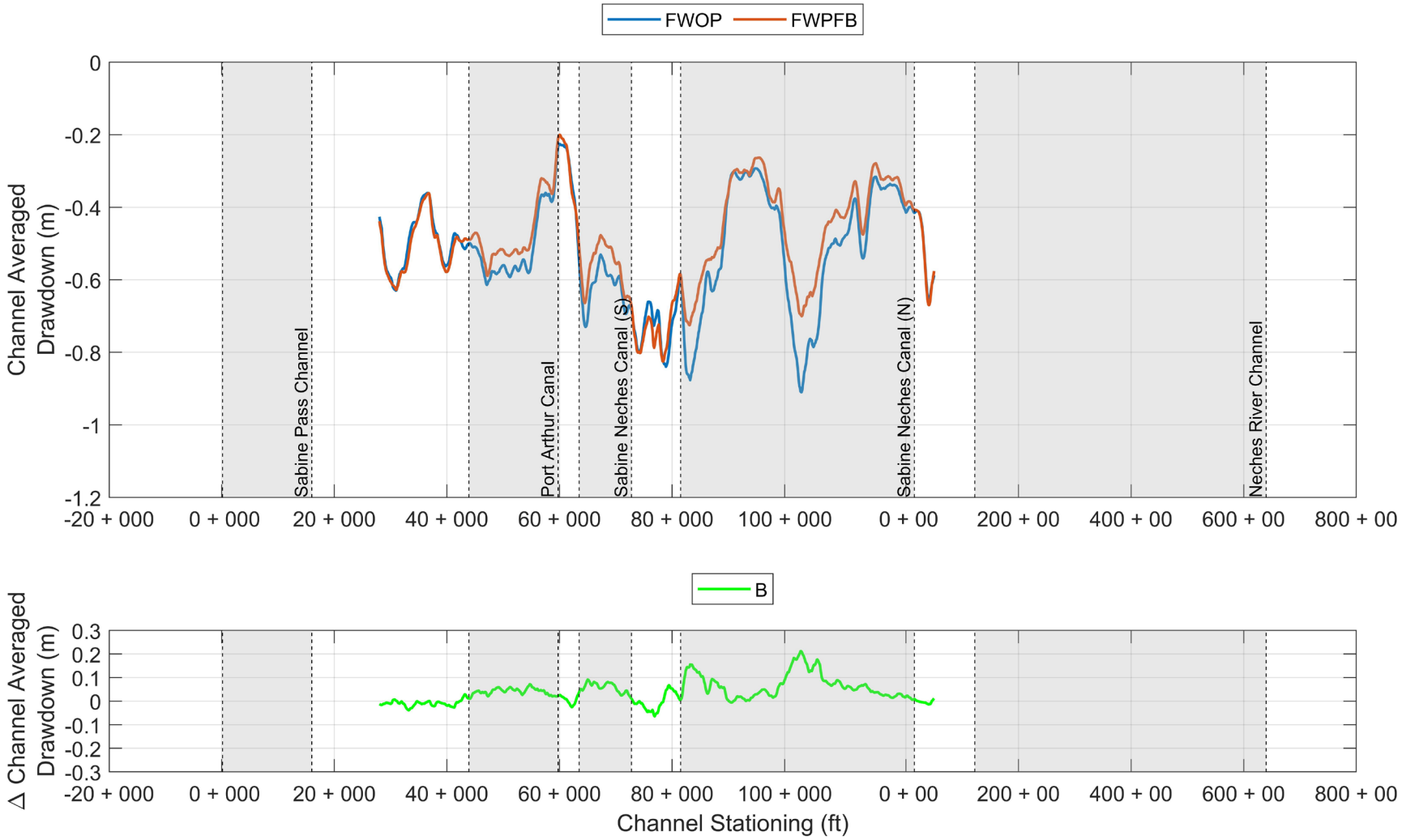

Figure 6-17
Channel Averaged Drawdown Versus Stationing from AdH Model for FWOP and FWPFB Including RSLC

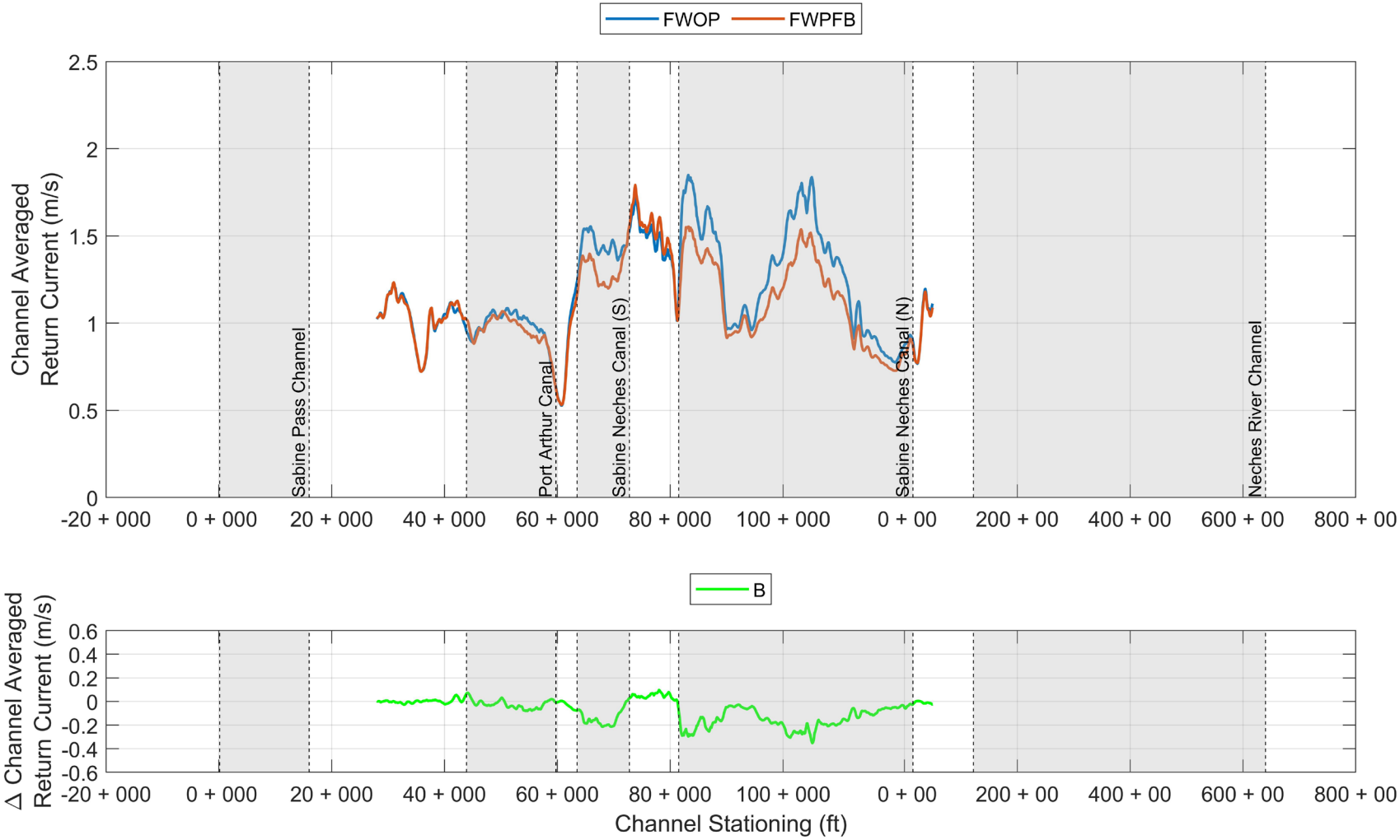

Figure 6-18
Channel Averaged Return Current Versus Stationing from AdH Model for FWOP and FWPFB Including RSLC

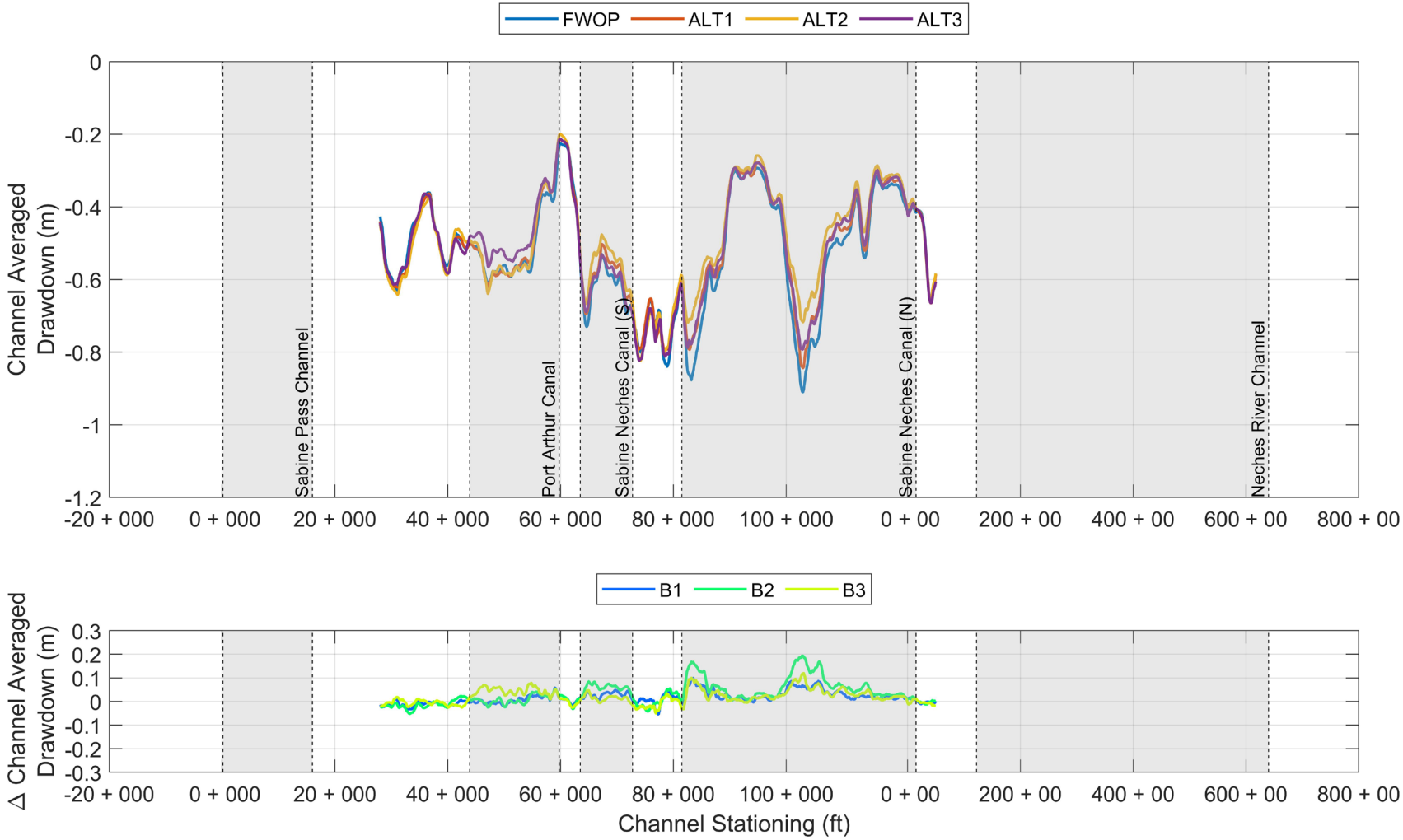

Figure 6-19
Channel Averaged Drawdown Versus Stationing from AdH Model for FWOP, ALT1, ALT2 and ALT3 Including RSLC.

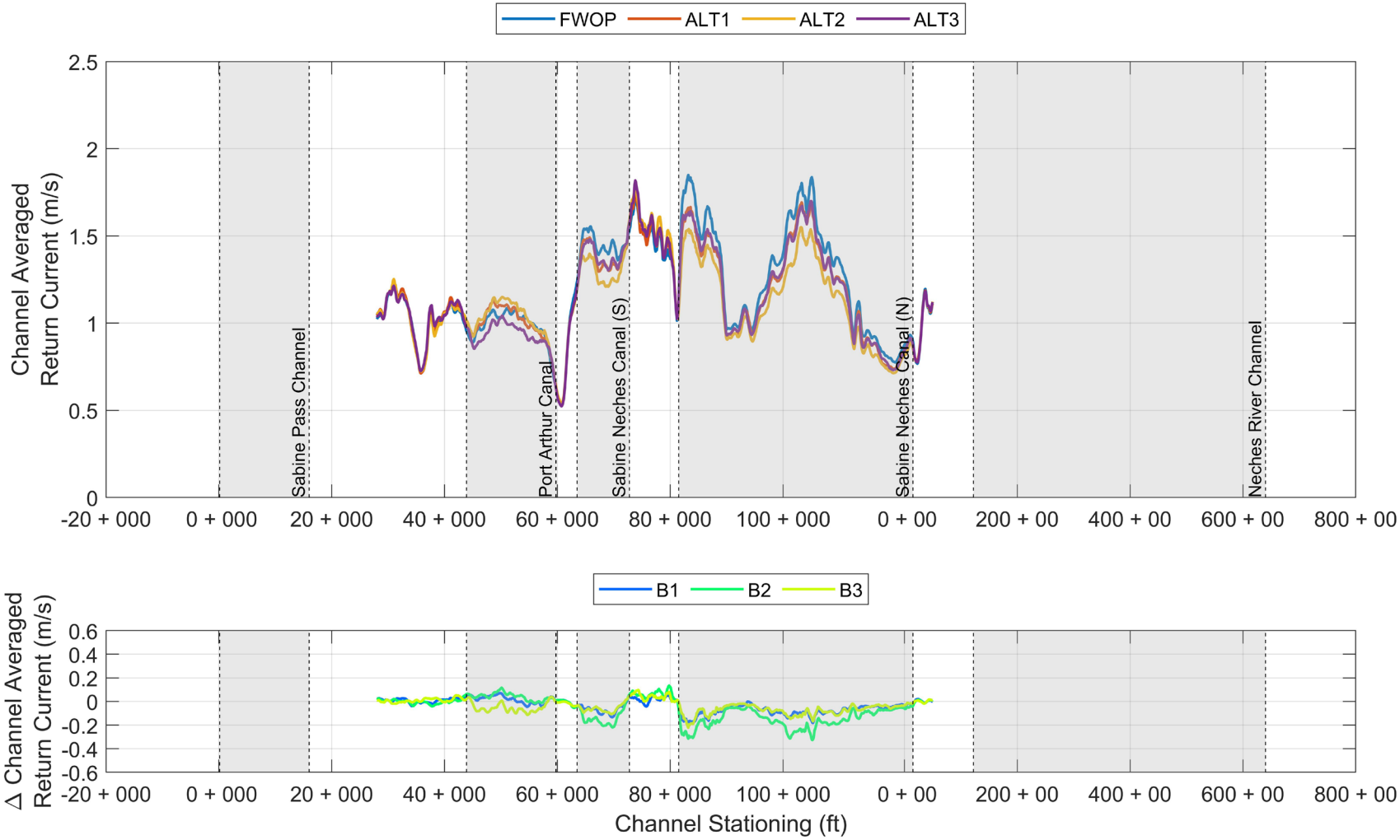

Figure 6-20
Channel Averaged Return Current Versus Stationing from AdH Model for FWOP, ALT1, ALT2 and ALT3 Including RSLC

Overall trends were analyzed by averaging the channel averaged drawdown and return current over the portion of the SNWW within the central mesh. The bulk results are given in Table 6-11, where the analysis from Section 6.2 is repeated for the limits of the central mesh only and included for reference. The channel averaged drawdown and return current were the largest for the FWOP scenario at 0.7 m and 1.5 m respectively. Including RSLC, these averages reduced to 0.5 m and 0.12 m respectively. Differences between channel conditions are presented in Table 6-12 following the comparisons B as described in Section 4.5 and detailed in Figure 4-5. Comparison B, B1, B2 and B3 all show no change or a reduction in drawdown and return current for both with and without RSLC. These results indicate the plan widening measures detailed in Section 3 reduce the magnitude of vessel hydrodynamics in Sabine Neches Canal when compared to the base FWOP condition.

Table 6-11
Modeled Channel Averaged Drawdown and Return Currents Averaged Along SNWW Reaches in the Central Mesh Only and Including RSLC

	FWOP	FWPFB	ALT1	ALT2	ALT3
Drawdown (m)	0.7	0.6	0.6	0.6	0.6
Drawdown RSLC (m)	0.5	0.5	0.5	0.5	0.5
Return Current (m/s)	1.5	1.3	1.4	1.4	1.4
Return Current RSLC (m/s)	1.2	1.1	1.2	1.1	1.2

* Note: Variances smaller than the Mean Absolute Model Error of 0.15 m and 0.1 m/s are not precise (calculated in Section 5.4).

Table 6-12
Differences in Modeled Channel Averaged Drawdown and Return Currents Averaged Along SNWW Reaches in the Central Mesh Only and Including RSLC.

	B	B1	B2	B3
Drawdown (m)	-0.1	0.0	-0.1	0.0
Drawdown RSLC (m)	0.0	0.0	0.0	0.0
Return Current (m/s)	-0.1	-0.1	-0.1	-0.1
Return Current RSLC (m/s)	-0.1	0.0	-0.1	0.0

* Note: Variances smaller than the Mean Absolute Model Error of 0.15 m and 0.1 m/s are not precise (calculated in Section 5.4).

6.5 Surge Portion of Transverse Stern Wave

The modeling performed in Maynord (2003) also did not reproduce the full transverse stern wave referred to as the "surge" that extends above the still water level. Generally, this type process

would be better captured by a phase-resolved wave model, which would also not be appropriate for evaluating the drawdown and return current. Therefore, this report evaluated the surge portion of the TSW empirically following the approach from Maynord (2003) shown in the below equation:

$$\frac{H_s}{h_b} = 0.26\left(\frac{d}{h_b}\right)F_b^{1.8} \quad (5)$$

Where,

$H_s =$ surge

$d =$ drawdown

$h_b =$ depth over the bank

$F_b =$ bank Froude number defined as $\frac{V}{\sqrt{gh_b}}$

$g =$ acceleration of gravity

$V =$ vessel velocity

The modeled vessel speed and drawdown from the time series comparison points (Section 6.1) were input from the model. Although these drawdown magnitudes were extracted at 3.5 m depth from the AdH modeling, they were analyzed in the surge equation 5 at the 1.5 m depth. The shallower analysis depth was used to yield peak surge magnitudes (bank Froude close to 1). Results of the analysis are shown in Table 6-13, showing surge heights ranging from 0.1 to 0.4 m. These surge heights equate to 10 to 20 percent of the computed drawdowns and follow the same trends between the base and plan conditions as the rest of the analysis presented in Section 6.

Table 6-13
Surge portion of transverse stern wave calculated at the 1.5 m depth contour

Reach	Station	Surge (m)					
		Existing	FWOP	FWPFB	ALT1	ALT2	ALT3
		(36 ft)	(44 ft)	(44 ft)	(44 ft)	(44 ft)	(44 ft)
Sabine Pass Channel	5+000	0.2	0.2	0.2	0.2	0.2	0.2
	12+500	0.1	0.1	0.1	0.1	0.1	0.1
Port Arthur Canal	32+500	0.2	0.2	0.2	0.2	0.2	0.2
	50+000	0.2	0.3	0.2	0.3	0.3	0.2
	55+000	0.2	0.3	0.2	0.2	0.3	0.2
Sabine-Neches Canal	67+500	0.2	0.3	0.2	0.2	0.2	0.2
	85+000	0.2	0.3	0.3	0.3	0.3	0.3
	105+000	0.3	0.4	0.2	0.3	0.2	0.3
Neches River Channel	250+00	0.2	0.2	0.3	0.2	0.3	0.2
	550+00	0.3	0.3	0.3	0.3	0.3	0.3
Mean:		0.2	0.3	0.2	0.2	0.2	0.2

Table 6-13 shows the transverse stern waves for all 10 of the analysis stations and for all of the channel configurations. Comparing the values from FWOP to the proposed widening scenarios results in a 0.1 m decrease for the FWPFB, ALT1, ALT2, and ALT3 channel conditions. Model Absolute Error of 0.15 m is still relevant in this analysis because drawdown is an input to the equation and was determined from the model results. Overall, the model results show similar trends to all analyses considered in this report which support a small (within model absolute error) decrease in vessel hydrodynamics.

6.6 Bank Erosion

The 2011 FEIS (USACE, 2008) explicitly evaluated bank erosion per passing vessel event using shear stress and a calibration factor. This analysis was used to extrapolate the total bank erosion over the project design life factoring in increased vessel traffic and changes to fleets calling to the SNWW. Because the proposed widening analyzed in this report will not modify the number or size of vessels calling to the SNWW this analysis was focused on qualitative comparisons of vessel hydrodynamics. Vessel hydrodynamics theory and the modeling presented in this report support that the widening will result in small to no changes to the vessel hydrodynamics in the SNWW. Therefore, the vessel hydrodynamics are not expected to change the bank recession.

It should be considered that the channel widening will push the channel closer to the existing channel bank, or even cut into the channel bank and place the widened channel adjacent to the new channel bank in some locations. However, during normal vessel transiting the vessels are expected to remain close to the channel center and therefore will not increase the vessel hydrodynamics along the bank.

7 Conclusions

A series of AdH model scenarios were developed to investigate the influence of widening portions of the SNWW channel on vessel generated hydrodynamics. Model results for the EC, FWOP, FWPFB, ALT1, ALT2, and ALT3 conditions are compared based on peak vessel-generated hydrodynamics. Several additional simulations were also compared for future with-project conditions and predicted RSLC. The results presented in Section 6 generally follow the expectations from theory, such as:

- Increasing both the channel cross-sectional area and the vessel draft while holding the speed fixed as a constant percentage of the theoretical limiting speed leads to a small increase in predicted changes to drawdown and return currents. (Comparison A).
- Increasing the size of the cross-sectional area of channel while keeping the vessel speed and draft fixed leads to a reduction in predicted changes to drawdown and return currents (Comparison B).
- Because the number and type of vessels calling on the SNWW are not expected to change due to the channel widening, and the vessel hydrodynamics are expected to remain the same or minimally decrease, the bank erosion is not expected to increase as a result of the channel widening.

In general, a deeper and wider channel will reduce vessel effects for the same vessel size, draft, and speed as explained by the physics of the Schijf equations (See section 1.2 and limit speed

below). This finding is consistent with the finding of the SNWW CIP feasibility study (USACE, 2008) where increased channel area was projected to reduce erosion effects. These results suggest that the widened channel will tend to reduce the vessel effects relative to FWOP for Suezmax class vessels with the same speed and draft. These findings are also consistent with those from the SNWW CIP feasibility study (USACE, 2008).

References

Berger C. and L. Lee (2005) Modeling of Vessel Effects: Selection of Adaption Parameters for Modeling Vessels in ADH. ERDC/CHL CHETN-IX-15. U.S. Army Corps of Engineers.

Berger R.C., J.N. Tate, G.L. Brown and G. Savant (2010). Adaptive Hydraulics A Two-Dimensional Modeling System Developed by The Coastal and Hydraulics Laboratory Engineer Research and Development Center User's Manual - AdH Version 3.2. Guidelines for Solving Two-Dimensional Shallow Water Problems with The Adaptive Hydraulics Modeling System.

Cooperative Institute for Research in Environmental Sciences (CIRES) at the University of Colorado, B. (2014). Continuously Updated Digital Elevation Model (CUDEM) - 1/9 Arc-Second Resolution Bathymetric-Topographic Tiles. TX N 29.5-30, W 94.25-93.5. NOAA National Centers for Environmental Information. https://doi.org/10.25921/ds9v-ky35. Accessed 08/25/2020.

Federal Emergency Management Agency (FEMA). (2011). Flood Insurance Study: Coastal Counties, Texas: Scoping and Data Review. Joint Report prepared for Federal Emergency Management Agency by the Department of the Army, U.S. Army Corps of Engineers. Washington DC.

Hammack, E. S. (2008). Modeling Vessel-Generated Currents and Bed Shear Stresses. ERDC/CHL TR-08-7. Vicksburg, Mississippi: U.S. Army Engineer Research and Development Center.

Huval C.J. (1980). Lock Approach Canal Surge And Tow Squat At Lock And Dam- 17 Arkansas River Project. Mathematical Model Investigation. Hydraulics Laboratory, U. S. Army Engineer Waterways Experiment Station. Vicksburg, MS.

Jansen, P. Ph., and Schijf, J. B. (1953). 18th International Navigation Congress, Rome, Permanent International Association of Navigation Congresses, Section 1, Communication 1, 175-197.

Maynord, S. (2003). Ship effects before and after deepening of Sabine-Neches Waterway, Port Arthur, Texas. ERDC/CHL TR-03-15. Vicksburg, Mississippi: U.S. Army Engineer Research and Development Center.

National Research Council (NRC) (1987) Responding to Changes in Sea Level: Engineering Implications. Washington, DC: National Academy Press. http://www.nap.edu/catalog.php?record_id=1006

PIANC. (1987). Guidelines for the Design and Construction of Flexible Revetments Incorporating Geotextiles for Inland Waterways, Supplement to Bulletin 57, Permanent International Association of Navigation Congresses, Brussels.

U.S. Army Corps of Engineers. (2006). Hydraulic Design of Deep-Draft Navigation Projects. (EM 1110-2-1613).

U.S. Army Corps of Engineers. (2008). Sabine-Neches Navigation Channel Improvement Project Final Engineering Appendix. Galveston District, Southwestern Division.

U.S. Army Corps of Engineers. (2011). Final Feasibility Report for Sabine-Neches Waterway Channel Improvement Project Southeast Texas and Southwest Louisiana Volume I. Galveston District, Southwestern Division.

U.S. Army Corps of Engineers. (2016). ER 1165-2-209. Water Resource Policies and Authorities Studies of Water Resources Development Projects by Non-Federal Interests. Washington, DC: Department of The Army.

U.S. Army Corps of Engineers. (2017). Sabine Pass to Galveston Bay, Texas Coastal Storm Risk Management and Ecosystem Restoration Final Integrated Feasibility Report - Environmental Impact Statement. Galveston District, Southwestern Division. U.S. Army Corps of Engineers (2018). Army Civil Works Program FY 2019 Work Plan – Construction. https://www.usace.army.mil/Missions/Civil-Works/Budget/

U.S. Army Corps of Engineers. (2019). Houston Ship Channel Expansion Channel Improvement Project Final Integrated Feasibility Report Environmental Impact Statement. Galveston District, Southwestern Division.

U.S. Army Corps of Engineers. (2019a). ER 1100-2-8162. Incorporating Sea Level Change in Civil Works Programs. Washington, DC: Department of the Army.